International Journal of Earth Sciences Knowledge and Applications
journal homepage: http://www.ijeska.com/index.php/ijeska

Research Article

e-ISSN: 2687-5993

Petrography and Geochemical Characterization of the Neoproterozoic Migmatites Around Mararraban Liman Katagum, Bauchi Nigeria

Tahir Garba Ahmad[1]*, Ahmed Isah Haruna[1], Faisal Abdullahi[1], Fatima Ibrahim Maikore[2]

[1]*Department of Applied Geology, Abubakar Tafawa Balewa Univeristy, Bauchi, Nigeria*
[2]*Investment Promotion and Mineral Trade Department, Ministry of Mines and Steel Development, Abuja, Nigeria*

INFORMATION

Article history
Received 24 December 2021
Revised 16 January 2022
Accepted 17 January 2022

Keywords
Migmatite
Metatexite
Diatexite
Petrograhy
Geochemistry

Contact
*Tahir Garba Ahmad
Tahirgarba967@gmail.com

ABSTRACT

The migmatitic rocks exposed around Mararraban Liman Katagum, Bauchi Nigeria were studied with a view to determine the Geology, petrography, geochemistry and morphology. The area has various morphological units of migmatites. metatexites occurring as patchy metatexite, diatexites as melanocratic diatexite, mesocratic and leucocratic diatexite. They have various flow structures of ptygmatitic folding that are induced by magmatic flow and this morphological forms of migmatite are associated with one another. Petrographic analysis shows metamorphic mineral assemblage comprises of quartz + plagioclase + biotite ± Microcline ± Muscovite ± orthopyroxene ± silliminite ± garnet ± accessory minerals and a typical abundance of quartz and biotite. The presence of metamorphic optical properties such as undulous extinction in quartz and obliteration of twinning in feldspar, and microstructure such as mymerkite, perthite indicate the rocks were subjected to pressure and temperature, and that partial melting is the main process that form the different suites of migmatitic rocks of the study area. Geochemically, a slight inverse correlation between SiO_2 and few elements is observed. This suggests that the classic model of fractional crystallization is not the principal process influencing the lithological diversity but partial melting in which the correlation patterns are controlled by the geochemistry of the solid phases been added to the melt. Various models were used to determine the ancestry of the migmatite in the study area. In all the plots the migmatite fell within sedimentary/ metasedimentary field which suggests that the protolith of the migmatite are of sedimentary or metasedimentary rocks.

1. Introduction

Migmatite outcrop in all part of Nigeria, they belong to the termed Migmatite Gneiss Complex of the basement component of Nigerian Geology. Migmatites are the most widespread of the component units in the Nigerian basement, which makes up about 60% of the surface area of the Nigerian basement (Rahaman and Ocan, 1978). They are the least understood and most understudied unit of the Nigerian basement. The study area Mararraban Liman Katagum and environs forms part of the Nigerian Basement Complex of Bauchi area that forms part of the Neoproterozoic Trans-Saharan belt formed between 700 and 580 Ma by accretion of terranes between the converging West African Craton, the Congo Craton, and the East Saharan Block (Ferre and Caby, 2006). The study area (Fig. 1) Mararraban Liman Katagum and environs lies within latitudes $10^0$3'20.4"N and $10^0$7'00"N and longitudes 9^0 36'00"E and $9^0$40'30"E (Fig. 1), and forms part of sheet 149 Bauchi SW covering a total area of 42 km^2 on a scale of 1:25,000.

The area is accessible through the major road linking Bauchi to Dass, and the outcrops are accessible through minor roads and footpaths that give access to the remote areas within the study area. The area has medium-high (Fig. 2) level outcrops (590-660 m) of the different morphological forms of migmatite. This work would deal with the petrography, and geochemical characterization of the Neoproterozoic migmatites morphologies.

2. Geological Setting

The Nigerian Basement Complex is situated in the pre-drift mobile belt defined by Kennedy (1964) east of the West

African and Sao-Luis Cratons Northwest of the Congo and Sao-Franscisco Cratons which was affected by the 550 ± 100 Ma Pan-African Orogeny. The entire belt lies in the reactivated margin of the West-African Craton and the active Pharusian Continental margin (Burke and Dewey, 1972; Black and Girod, 1972; Caby et al., 1981). Nigeria is situated within the Pan African mobile belt and sandwiched between the West African Craton to the west, the Tuareq Shield to the north and the Congo Craton to the southeast (Fig. 3). About half of the total area of Nigeria landmass is underlain by rocks of the Precambrian age known in the country as the Basement Complex. The remaining half is covered by Cretaceous to Quaternary sediments and volcanics. The Nigerian basement was affected by the 600 Ma Pan-African orogeny and it occupies the reactivated region which resulted from plate collision between the passive continental margin of the West African craton and the active Pharusian continental margin (Burke and Dewey, 1972; Dada, 2006).

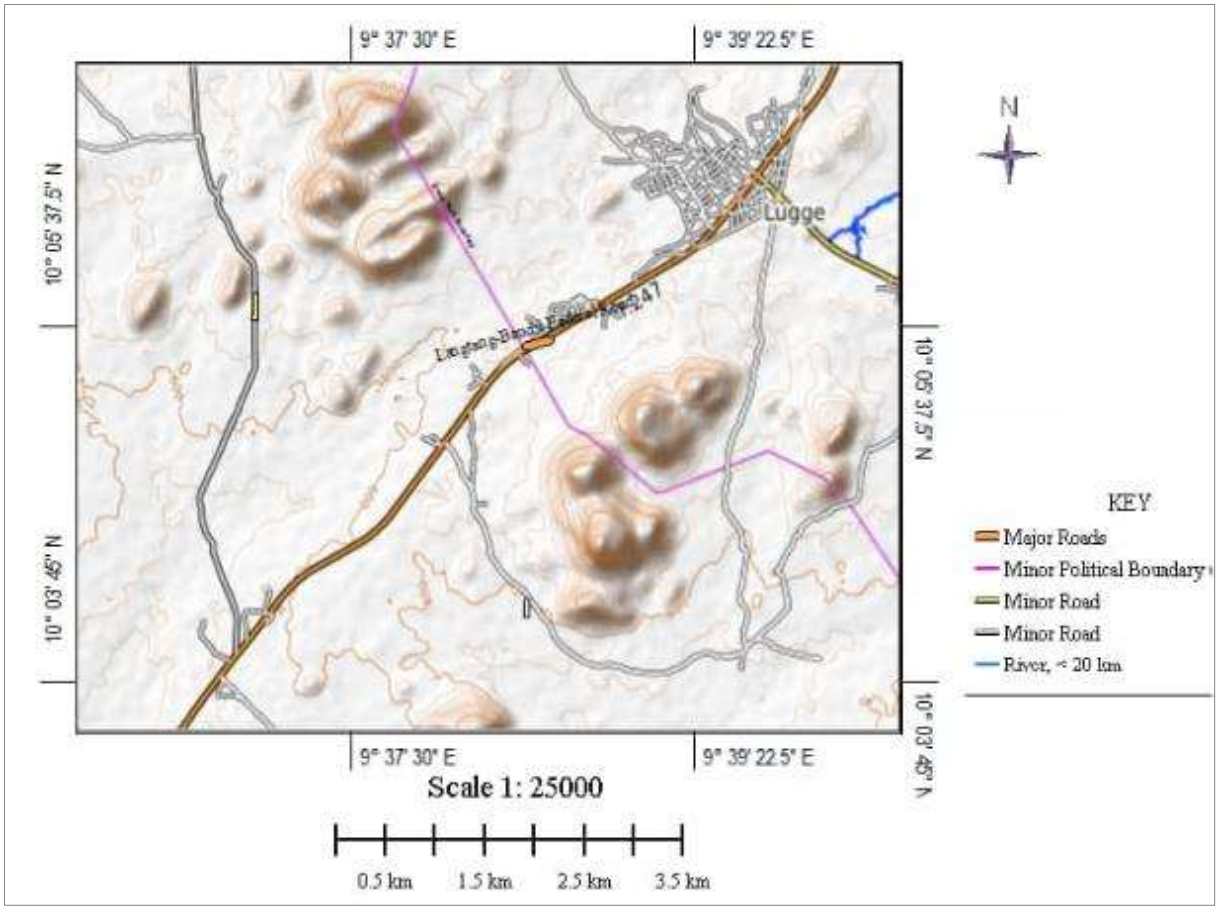

Fig. 1. Topographic map of the study Area (Source: Google earth)

The basement rocks are believed to be the results of at least four major orogenic cycles of deformation, metamorphism and remobilization corresponding to the Liberian (2,700 Ma), the Eburnean (2,000 Ma), the Kibaran (1,100 Ma), and the Pan-African cycles (600 Ma). The first three cycles were characterized by intense deformation and isoclinal folding accompanied by regional metamorphism, which was further followed by extensive migmatization.

The Pan-African deformation was accompanied by a regional metamorphism, migmatization and extensive granitization and gneissification which produced syntectonic granites and homogeneous gneisses (Abaa, 1983). Late tectonic emplacement of granites and granodiorites and associated contact metamorphism accompanied the end stages of this last deformation. The end of the orogeny was marked by faulting and fracturing (Gandu et al., 1986; Olayinka, 1992). The evolution of the Nigerian Basement Complex during the late Proterozoic is considered to be related to the activities taking place at the plate boundary. Initial crustal extension and continental rifting at the West African craton margin about 100 Ma ago led to the formation of graben-like structure in western Nigeria and subsequent deposition of the rocks of the schists belt. Nigerian Basement rocks from radiometric ages indicate that their evolution took place over at least four orogenic; Liberian (2,700 ± 200 Ma), Eburnean (2,000 ± 200 Ma) which is believed to form the Eburnean granite and metamorphic rocks with associated Proterozoic supracrustal, low grade metasedimentary, and meta-volcanic rocks, Kibarian (1,100 ± 200 Ma) and Pan-African (600 ± 150 Ma) (Black et al., 1979; Caby et al., 1981).

According to McCurry (1989), the Pan African orogeny was responsible for an extensive modification of the original rocks through metamorphism, migmatization and gneissification which precede syntectonic granite and homogenous gneisses (Abaa,1983). The migmatites have been found cutting across all the geologic ages above.

The basement complex is divided into two provinces (Ajibade et al 1979). The Western Province and the Eastern province. The Western Province is approximately west of longitude 8ºE, typified by N-S to NNE-SSW trending schist belts separated from one another by migmatites, gneisses and granites. This trend is believed to be the result of Pan African orogeny involving collision between the West African Craton and the Pan African mobile terrain with and eastward dipping subduction zone. The schist belts are differently interpreted as small ocean basins (Ajibade et al, 1989) infilled rift structures (Ball, 1980) or synclinal remnants of an extensive supracrustal cover (Barley et al, 1989). The Eastern Province lies approximately east of longitude 8ºE and is more nearly NE-SW. When followed eastward into Cameroon, the trend changes to ENE-WSW (e.g Ngaoundere, mylonite zone and the schist belts near Batare).

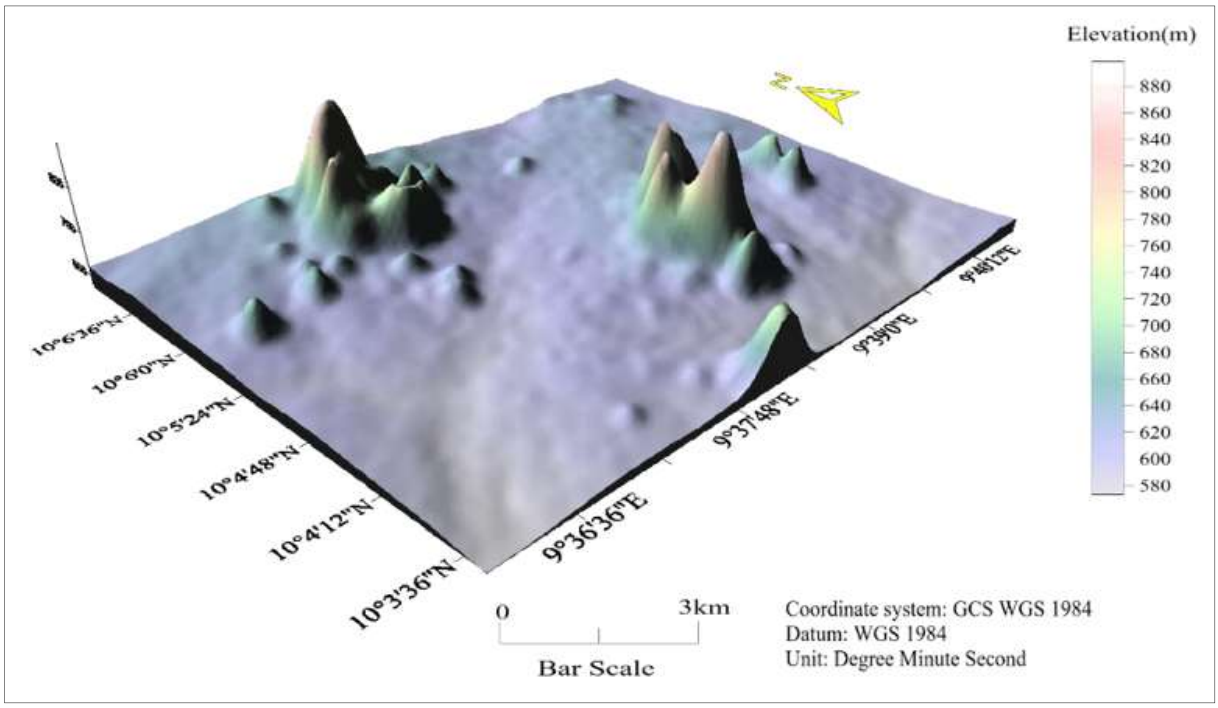

Fig. 2. Digital elevation model of the study area (Surfer 13)

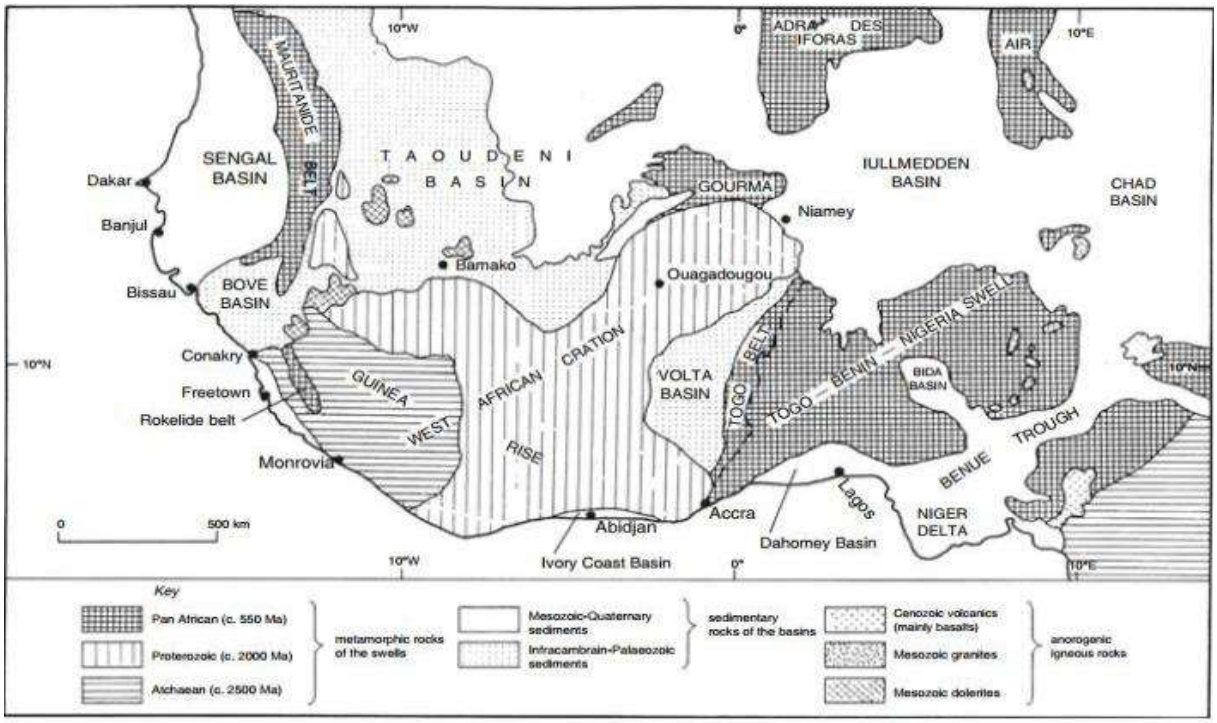

Fig. 3. Geological map of parts of West Africa showing the position of Nigeria and its Pan- African basement, the Congo-Gabon craton, the West African craton and the Tuareg Shield (adapted from Wright et al., 1985)

The Eastern Province comprises mainly migmatites, gneisses and large masses of Pan-African granitoids (Older Granites) intruded in Jos plateau, by Jurassic peralkaline granites. Except for smaller schist occurrences around Madagali (Hawal Massif), Toungo and Gayam (Adamawa Massif) and Oban Massif in southeast, the Eastern Province is marked by the absence of major schist belts. Precambrian Basement Complex rocks underlie three areas of Nigeria: North-central area including the Jos Plateau; South-west area adjacent to Benin; and south-east area adjacent to Cameroon. The rocks of the North-central area are composed of gneisses, migmatites, granites, schists, phyllites and quartzites.

The narrow, tightly folded north-south trending schist belts of northwestern Nigeria include igneous rocks, pelitic schists, phyllites and banded ironstones. The migmatite-gneiss complex of amphibolites, diorites, gabbros, marbles and pegmatites form a transition zone between the schist belt of NW Nigeria and the granites of the Jos Plateau to the east. There, extensive Precambrian Age Older Granites crop out extensively. These have been intruded by Jurassic age Younger Granites that for characteristic ring complex structures.

The Precambrian Basement rocks of southwestern Nigeria, as found in the Dahomey (Benin) Basin, consist of migmatites, banded gneisses and granite gneisses, with low grade metasedimentary and metavolcanic schists, intruded by Pan-African age granites and charnockites (Oyawoye, 1972). The migmatites and gneissic metasediments are often intruded by pegmatite veins and dyke. Older granites, granodiorites and syenites, with dolerite dykes, also form part of the Precambrian basement of SW Nigeria. The Precambrian Basement rocks of south-eastern Nigeria occur in three blocks along the border with Cameroon. The crystalline basement rocks include biotite-hornblende gneiss, kyanite gneiss, migmatite gneiss and granites and are well fractured.

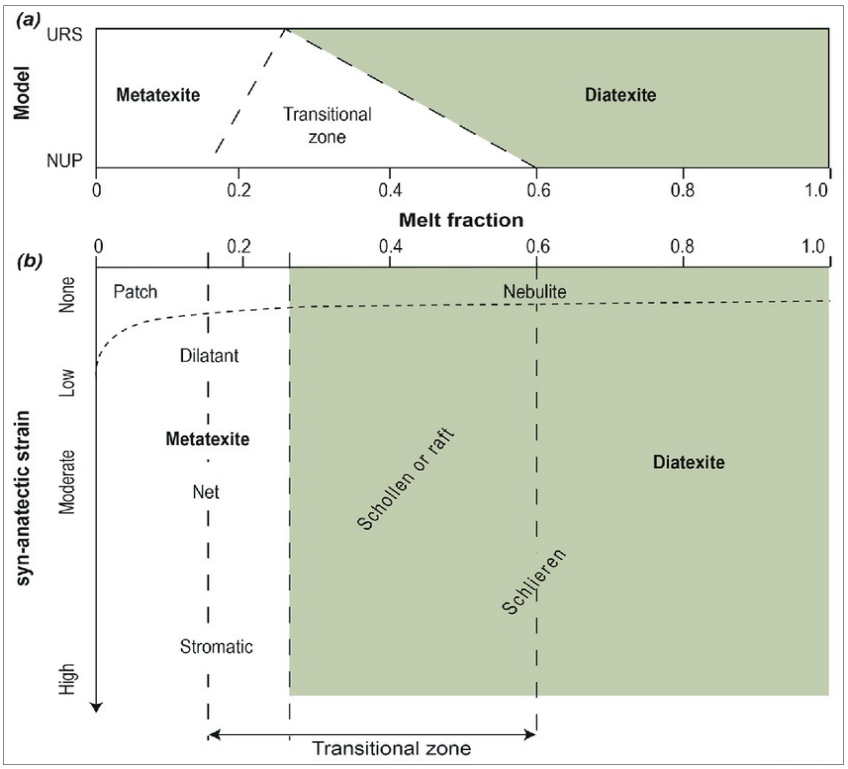

Fig. 4. Classification scheme for migmatitic rocks modified from Sawyer (2008); a) First-order division of migmatites into metatexite and diatexite migmatites as a function of the fraction of melt and the properties of the solid grains in the partially melted rock and b) Second-order morphologies of metatexite and diatexite migmatites on a plot of syn-anatectic strain versus melt fraction. The diagram is shaded for the URS model but the vertical dashed lines indicate where the boundaries are for the transitional zone

2.1. Morphology of migmatites

Sederholm (1907) introduced the term migmatite for the new rocks formed where an older foliated granite was intruded by the younger Hango granite in Finland. In his detailed description of the changes that had occurred to the older granite, Sederholm used terms such as "reborn" and "new eruptivity" (at the time, "eruptivity" meant "intrusivity") to explain what he saw. From these terms it is evident that in 1907 he thought that partial melting was the principal process involved in the formation migmatite. In the same paper Sederholm (1907) introduced the term anatexis to describe the general case (i.e., without restriction as to the degree of melting) of partial melting in the crust. In his later works, however, Sederholm (1923, 1926) placed more emphasis on the role of fluids and of assimilation in the formation of migmatites.

Migmatites form under extreme temperature and pressure conditions during prograde metamorphism, when partial melting occurs in metamorphic paleosome (Mehnert, 1971;

Frost et al., 2001), components exsolved by partial melting are called neosome (meaning 'new body'), which may or may not be heterogeneous at the microscopic to macroscopic scale. Migmatites can be divided into two first-order groups; metatexites and diatexites. Metatexites are migmatites that preserve coherent, pre-partial melting structures in the palaeosome and residuum whereas diatexites have disaggregated and lost structural coherency (Sawyer, 2008).

Sawyer (2008) describes four main second order divisions of metatexite; patch, dilational, net and stromatic. However, it is important to remember that there is a progression and there can be overlaps between these structural types. For example, the development of shear bands can cause a stromatic migmatite to develop net type structures, it is important to remember that these represent transitional stages as the rock progresses to high degrees of partial melt and complete disruption of the protolith (Fig. 4).

3. Materials and Method

Geological mapping of the area was conducted on a scale of 1: 25,000. Particular attention was taken for the location, physical characteristics structural elements and associated rocks of the migmatites. Various field measurements were used during the mapping. Global Positioning System (GPS) was used for geographical positioning with respect to various outcrops available in the study area. Field descriptions and observation were adequately recorded in a field notebook.

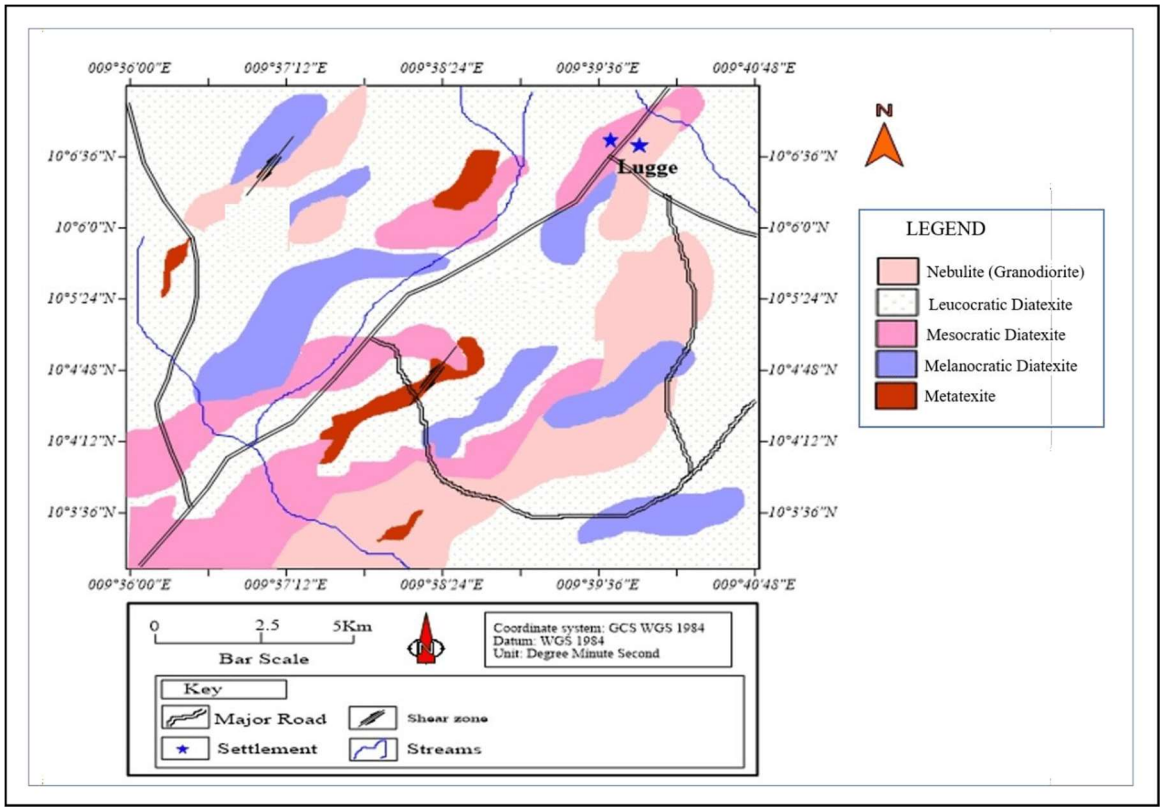

Fig. 5. Geologic map of the study area

The sample sorting was carried out using Sawyer (2008) first- and second-order morphological classifications of migmatite. Representative sample was selected for petrography and Geochemical analysis. For the petrographic studies, the rock samples were cut into chips with a microcutting machine and subsequently polished on glass ground plate using carborundum to obtain required thickness and a perfectly smooth surface; the cut rock samples were, thereafter, mounted on a clean glass slide with adhesive. The prepared slides were examined under the petrological microscope to identify mineralogical features of the rock samples on a microscopic scale. Same samples were. The same representative rock samples were taken to Research and Development (R&D) Laboratory of the Nigerian Geological Survey Agency Kaduna, for sample preparation and analysis. Geochemical analysis of the samples was conducted at Geological Survey Agency Laboratory, for major oxides and trace elements composition determination, using Energy Dispersive X-ray Fluorescence Spectrometry (EDXRF). Geochemical data were processed using Petrograph and GCDKit software package for different geochemical variation and discrimination diagrams.

4. Results and Discussion

The study area is underlain by two lithomorphological form of migmatite, metatexite and diatexites. The metatexites in the study area occur as patch metatexites. This texture is seen when melting occurs at discrete sites to form small, scattered patches of non-foliated in situ neosome. patch migmatites are rare and in this case they occur with diatexites as patches. They are dominated by paleosome and are characterized by the occurrence of small scattered patches of leucosome

resulting from discrete partial melting. The diatexites found in the study area show a considerable range in morphology from mesocratic to melanocatic through to leucocratic diatexites. The nebulite occur as boulders along the Mesocratic and Leucocratic diatexite in the field (Fig. 5).

4.1. Field relationship, macroscopic and microscopic description metatexite

The metatexite within the study area occur as patch metatexite and they occur as patches within the leucocratic diatexite. They are residuum rich rocks which are dominated by the paleosome. They are characterized by the occurrence of small scattered patches of leucosome within the patch metatexite (Fig. 6).

The patch metatexite occurs as patch within the mesocratic diatexite. It is fine grained and is residuum rich rock predominant of paleosome. It contains a lot of dark colored mineral and light spot that is possible is quartz. It has no evidence of any layering (Fig. 7).

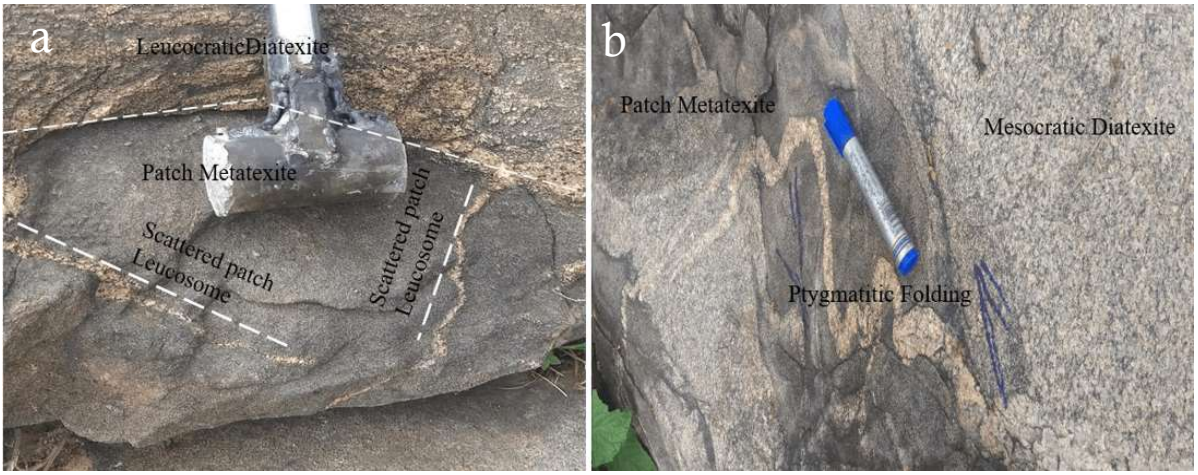

Fig. 6. Field occurrence/ Morphology of the metatexite showing small scattered patches of leucosome and ptygmatic folding occurring within a Mesocratic diatexitic body

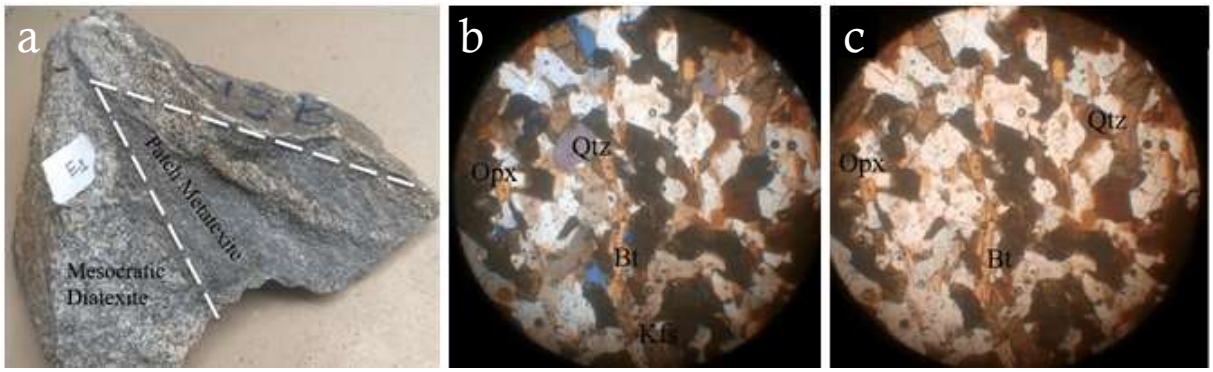

Fig. 7. Hand Sample of the patch metatexite (sample E1) (a) and photomicrograph of metatexite (sample E1) under both PPL (b) and XPL (c) (Qtz: Quartz, Bt: Biotite, Opx: Orthopyroxene)

Table 1. General optical properties of the melanocratic diatexites under plane and crossed polarised light

Minerals	PPL	XPL
Quartz	Quartz is colorless with low relief and no cleavage under PPL	Wavy undulose extinction indication of dislocation walls in mineral grains
Biotite	Perfect cleavage in one direction, and brownish to tan in color	Darker brown with one directional cleavage
Orthopyroxene	Orthopyroxene is greenish to pinkish pleochric	Pale green, moderate to high relief

4.1.1. Diatexite

The diatexites in the study area is the most widespread and abundant morphology in the study area. Unlike metatexite that occur as patches they occur as massive rock unit and are intricately associated with one another. All have undergone a textural homogenization that has destroyed the pre-migmatization structures (e.g., bedding and foliation). They are highly characterized by ptygmatitic folding (Fig. 8). These folds are magmatic fold and have no relationship or association with bedding or layering of the protolith. The diatexites found in the study area show a considerable range in morphology from mesocratic to melanocatic through to leucocratic diatexites and they are associated with one another (Figs. 8 and 9).

The occur as boulders (Fig. 9) along mesocratic and leucocratic diatexite but have no any distinguishable contact. It shows a complex relationship with the metatexites. The diatexites show a granitic appearance in most cases. In some cases, at outcrop level it shows elongation of the feldspar phenocryst (Fig. 9b).

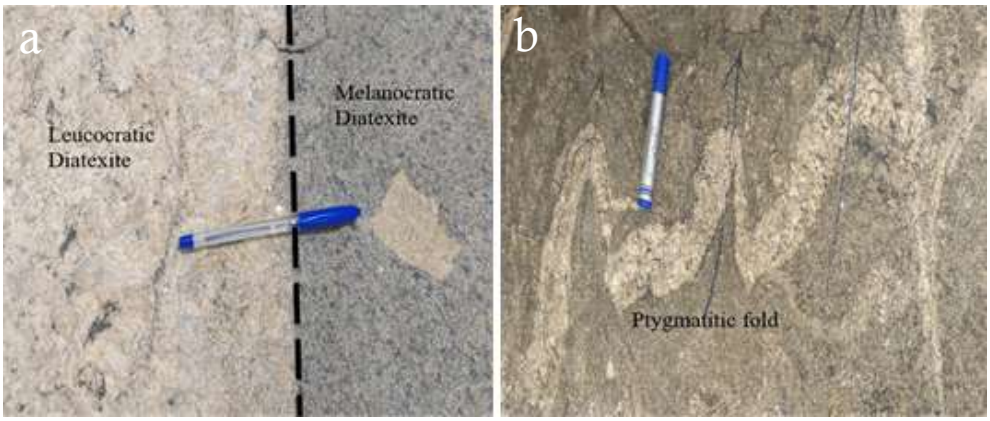

Fig. 8. a) Clear contact between the leucocratic diatexite and melanocratic diatexite as observed in the field and b) Mesocratic diatexite displaying ptygmatitic folding

Fig. 9. a) Contact between mesocratic diatexite and leucocratic diatexite in the field, b) Mesocratic diatexite forming large feldspar phenocryst and c) Granodiorite on outcrop scale, occurring as massive boulders

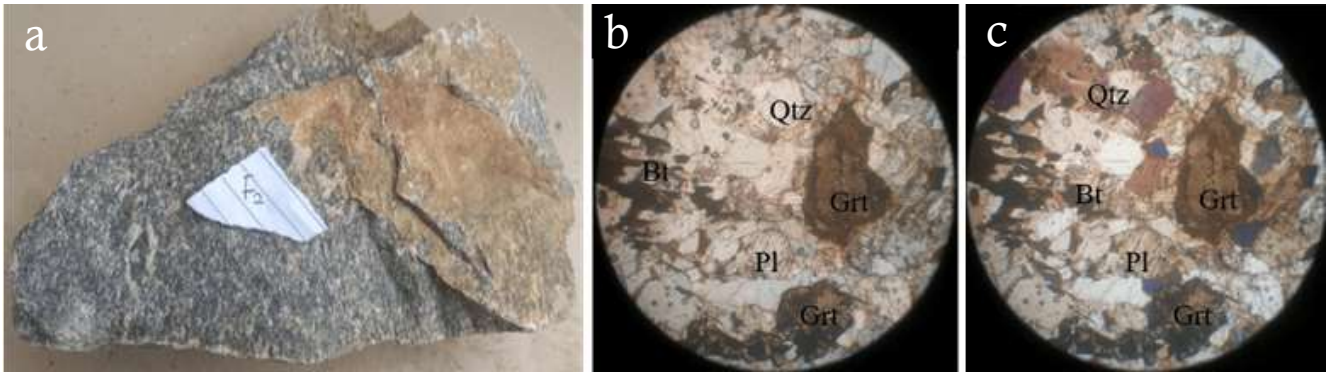

Fig. 10. Photograph of hand sample of melanoocratic diatexite (sample F2) (a) and photomicrograph of melanocratic diatexite (sample F2) under both PPL (b) and XPL (c) (Qz: Quartz, Bt: Biotite Grt: Garnet, Pl: Plagioclase)

Table 2. General optical properties of the melanocratic diatexites under plane and crossed polarised light

Minerals	PPL	XPL
Quartz	Quartz is colourless with low relief and no cleavage under PPL	Wavy undulose extinction indication of dislocation walls in mineral grains
Biotite	Biotite showing perfect cleavage in one direction, and brownish	Elongated platy brown with one directional cleavage
Garnet	Brownish subhedral grain	Pale greenish subhedral grain
Plagioclase	Plagioclase colourless	Twinning visible
Silliminite	Silliminite is colourless	Silliminite has second order interference colour, pale yellowish

4.1.1.1. Melanocratic diatexite (F2)

The melanocratic diatexite is medium to fine grained (0.5-1mm) and has high content of dark colored mineral with the light spot as quartz (Fig 10). The dark colored may be as a result of biotite content or high ferromagnesian minerals.

4.1.1.2. Mesocratic diatexite (E3)

The rocks are fine grained (0.5-2mm). They are composed of quartz, feldspar and biotite and have a strong preferred orientation of the biotite, suggesting a magmatic or submagmatic foliation.

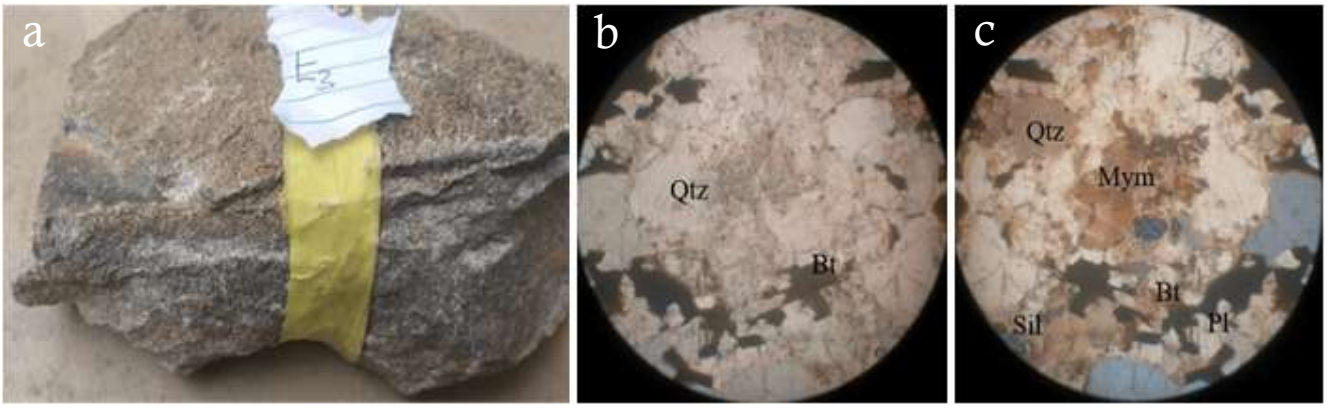

Fig. 11. Photograph of hand sample of mesoocratic diatexite (sample E3) (a) and photomicrograph of mesocratic diatexite (Sample E3) under PPL (b) and XPL (c) (Qtz: Quartz, Bt: Biotite, Sil: Silliminite, Mym: Mymerkite, Mc: Microcline)

Table 3. General optical properties of the mesocratic diatexites under Plane and Crossed polarised light

Minerals	PPL	XPL
Quartz	Quartz is colourless with low relief	Wavy undulose extinction that shows dislocation of wall in mineral grains
Biotite	Elongated platy brown biotite	Elongated platy brown biotite
Mymerkite	Mymerkite not visible under PPL	Mymerkite microstructure visible
Plgioclase	Twinning not visible under plane Polars in plagioclase	Twinning visible under cross polars in plagioclase
Silliminite	Silliminite is colourless	Silliminite shows pale yellowish

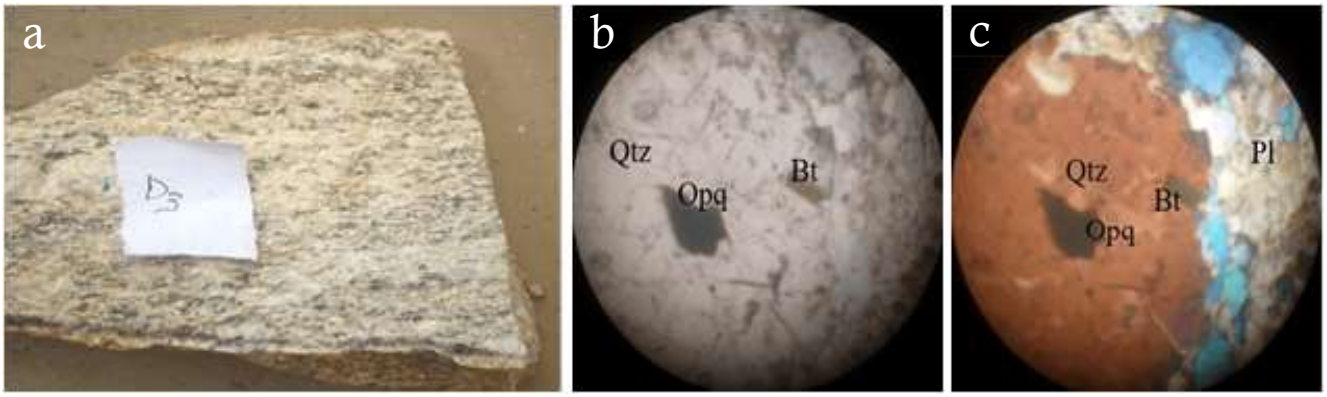

Fig. 12. Photograph of hand sample of leucocratic diatexite (sample D3) (a) and photomicrograph of leucocratic diatexite (Sample D3) under PPL (b) and XPL (c) (Qz: Quartz, Bt: Biotite, and Opq: Opaque)

Table 4. General optical properties of the leucocratic diatexites under Plane and Crossed polarised light

Minerals	PPL	XPL
Quartz	Quartz is colourless with low relief	Wavy undulose extinction
Biotite	Elongated platy brown	Elongated platy brown biotite
Opaque	Black opaque mineral	Black opaque mineral

4.1.1.3. Leucocratic diatexite (D3)

The rocks are fine grained (0.5-2mm). It is composed of quartz, feldspar and biotite and have a strong preferred orientation of the biotite, suggesting a magmatic or submagmatic foliation.

4.1.2. Nebulite (granodiorite)

The rock is coarse grained (2-10mm) and is composed of large grains of quartz and biotite. Morphologically the rock is nebulitic (Fig 13).

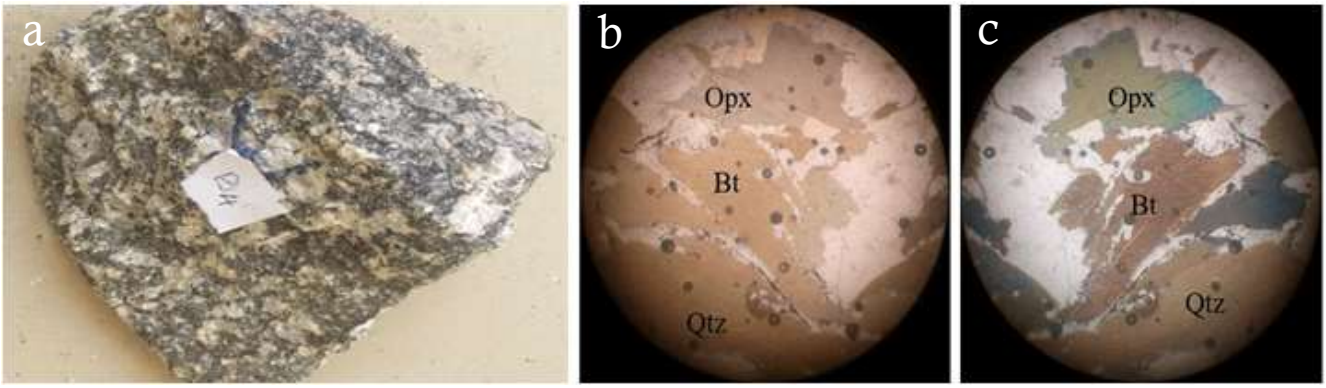

Fig. 13. Photograph of hand sample of nebulite (sample B4) (a) and photomicrograph of nebulite (Sample D5) under PPL (b) and XPL (c) (Qtz: Quartz, Bt: Biotite, Opx: Orthopyroxene)

Table 5. General optical properties of the leucocratic diatexites under plane and crossed polarised light

Minerals	PPL	XPL
Quartz	Quartz is colourless with low relief	Wavy undulose extinction that shows dislocation of wall in mineral grains
Biotite	Elongated platy brown biotite with perfect cleavage	Elongated platy brown biotite with perfect cleavage
Ortopyroxene	Orthopyroxene showing greenish colour	Orthopyroxene Showing greenish colour

Table 6. Whole-rock composition with major oxide expressed in weight% and trace element in ppm, of metatexite, melanocratic diatexite and mesocratic diatexite

Sample	A	E1	F2	F3	B1	B2	B3	C2	C3	C4	E1b
Oxide (wt %)	**Metatexite**		**Melanocratic diatexite**		**Mesocratic diatexite**					**Mesocratic diatexite**	
SiO_2	58.1	67.1	71.2	70.1	74.4	70.1	70.6	73.2	72.1	73.0	71.2
CaO	1.0	0.4	0.3	0.2	0.4	0.7	0.2	0.4	0.4	0.3	0.4
MgO	4.4	1.0	0.0	0.0	0.8	0.3	1.9	0.1	0.0	0.1	0.0
SO_3	0.0	0.0	ND	ND	ND	ND	0.0	ND	ND	ND	ND
K2O	0.2	0.6	3.4	1.4	1.2	2.4	1.3	1.0	1.3	1.2	0.8
Na_2O	0.5	1.8	1.8	2.0	0.7	2.0	2.0	2.0	2.0	1.9	2.0
TiO_2	2.2	1.4	1.5	2.0	1.0	1.0	1.0	1.0	1.6	1.0	0.8
MnO	0.0	0.0	0.1	ND	0.0	0.1	0.1	0.1	0.1	0.1	0.1
P_2O_5	0.1	ND	ND	ND	0.0	ND	ND	ND	ND	ND	ND
Fe_2O_3	18.2	12.4	8.0	10.1	3.7	7.8	4.6	8.0	7.1	4.4	6.6
Al_2O_3	13.2	12.2	13.6	12.8	14.8	13.6	14.0	12.9	13.2	13.4	13.4
H_2O	2.0	2.6	2.5	1.8	1.0	2.0	2.2	1.2	1.4	1.1	2.5
Trace element (PPM)											
V	686.0	702.0	601.0	482.0	622.0	530.0	420.0	534.0	420.0	660.0	420.
Cr	345.0	425.0	346.3	245.0	327.0	312.1	210.4	304.2	210.4	336.0	248.
Cu	310.0	290.0	334.0	334.0	360.0	160.0	280.0	180.0	280.0	380.0	330.
Sr	2030.0	290.0	1220.0	2031.0	493.0	120.0	1000.0	110.0	1000.0	1830.0	1220
Zr	1500.0	720.0	1200.0	150.0	2710.0	731.0	1000.0	730.0	1000.0	1200.0	1200
Ba	1800.0	100.0	3100.0	1810.0	6400.0	900.9	600.0	900.9	600.0	2010.0	3100
Zn	560.0	50.0	97.0	56.0	190.0	20.0	160.0	20.0	160.0	370.0	97.0
Ce	54.0	45.0	50.0	44.0	39.9	54.0	80.0	54.0	80.0	63.0	50.0
Pb	867.0	17.0	26.0	867.0	41.0	72.9	580.0	70.9	580.0	56.1	26.0
Bi	0.9	0.2	0.1	0.9	0.2	1.7	4.0	0.7	4.0	5.0	0.0
Ga	12.0	17.4	39.0	42.0	9.1	12.6	6.0	12.0	6.0	5.1	39.0
As	17.0	7.0	9.0	17.3	6.0	21.0	0.5	21.0	0.5	3.0	7.0
Y	3.9	39.0	15.0	3.9	20.0	24.0	26.0	24.0	26.0	4.3	15.0
Ir	6.1	3.1	20.0	6.1	1.0	28.0	3.8	28.0	3.8	2.0	20.0
Au	0.5	0.0	1.2	0.5	0.4	0.8	1.6	0.8	1.6	0.2	0.2
Ni	0.0	<0.001	<0.001	0.0	<0.001	0.0	<0.001	<0.001	<0.001	<0.001	<0.0
Rb	30.0	9.8	29.0	30.0	86.0	27.0	62.0	27.0	62.0	36.0	29.0
Mo	83.0	14.0	32.0	81.0	0.0	<0.001	0.0	<0.001	0.0	0.0	32.0
Co	0.2	0.0	<0.001	0.2	0.3	1.0	1.0	1.0	1.0	<0.001	<0.0
Cd	1.1	<0.001	0.0	1.1	0.0	0.0	<0.001	0.0	<0.001	0.0	0.0
Ru	<0.001	<0.001	0.0	0.001	8.7	5.1	1.0	5.1	1.0	1.2	0.1
Eu	2.1	0.8	0.1	2.1	31.0	57.0	23.0	7.0	23.0	340.0	0.1
Re	34.0	120.0	180.0	36.0	0.0	0.0	0.0	0.0	0.0	<0.001	180.
Nb	12.0	16.1	40.4	11.0	24.1	10.0	60.0	10.0	60.0	42.0	20.0
Ag	0.1	0.7	0.4	0.1	1.3	0.9	1.1	0.9	1.1	0.5	0.4
Ta	64.0	64.0	42.1	60.0	64.1	38.0	101.0	38.0	101.0	55.0	42.1
W	1.5	13.3	0.9	1.5	4.0	7.8	5.6	7.8	5.6	5.1	0.9
Hf	21.0	16.0	33.0	21.0	14.0	6.6	28.0	6.6	28.0	24.0	33.0
Yb	6.9	1.1	0.0	6.9	1.0	2.0	0.2	2.0	0.2	0.5	4.0
In	0.1	3.0	2.1	0.1	5.2	3.5	2.8	3.5	2.8	2.2	2.1

Se	0.0	0.3	0.0	0.0	0.3	0.1	0.2	0.1	0.2	0.3	<0.0
U	0.0	<0.001	<0.001	0.0	0.2	0.1	0.0	0.1	0.0	<0.001	<0.0
Th	2.2	0.8	2.5	2.2	0.2	0.2	0.1	0.2	0.9	0.3	2.5
Sb	14.0	12.7	7.0	14.0	0.3	0.6	2.2	0.6	2.2	3.3	7.2
Ge	40.0	24.0	24.0	40.0	80.6	34.4	18.8	14.4	8.8	4.4	220.
Sn	20.1	9.8	33.3	11.1	37.2	52.6	47.0	42.6	27.0	19.9	3.3

Table 7. Whole-rock composition with major oxide expressed in weight% and trace element in ppm, of Mesocratic Diatexite, Leucocratic Diatexite and Granodiorite (Nebulite)

Sample	**E3**	**E4**	**F1**	**C1**	**D1**	**D2**	**D3**	**D4**	**D5**	**B4**
Oxide (wt %)	**Mesocratic diatexite**			**Leucocratic diatexite**						**Granodiorite**
SiO_2	72.6	73.0	70.6	73.8	72.1	74.6	73.4	72.6	78.7	76.2
CaO	0.4	0.3	0.2	0.3	0.4	0.2	0.6	0.1	0.0	0.2
MgO	0.1	0.0	1.2	0.1	0.1	0.1	0.1	ND	ND	0.0
SO_3	0.0	ND	0.1	ND	ND	ND	ND	ND	ND	ND
K_2O	1.0	4.0	1.6	3.4	1.6	1.8	4.4	7.4	2.4	0.7
Na_2O	2.0	1.3	2.1	1.2	1.8	2.6	1.1	1.0	1.2	1.6
TiO_2	1.3	0.8	1.6	0.6	1.2	0.9	0.4	0.6	0.2	0.5
MnO	0.1	0.1	0.1	0.0	0.1	0.1	0.0	0.1	ND	0.0
P_2O_5	ND	ND	ND	ND	ND	ND	ND	ND	ND	ND
Fe_2O_3	5.2	4.4	6.7	4.5	4.6	3.4	3.0	2.5	1.7	6.4
Al_2O_3	14.2	13.8	13.4	13.2	14.6	13.8	13.1	13.6	12.6	13.1
H_2O	1.7	2.1	2.7	1.6	2.3	1.0	2.0	2.1	1.0	1.0
Trace element (PPM)										
V	611.0	386.0	422.0	520.0	720.0	401.0	383.0	498.1	510.0	321.0
Cr	326.3	145.0	217.0	317.0	412.1	245.3	114.2	210.1	330.2	112.1
Cu	344.0	310.0	360.0	360.0	240.0	334.0	379.0	460.0	340.0	415.0
Sr	1020.0	2030.0	493.0	493.0	1790.0	1220.0	980.0	1020.0	1450.0	2230.0
Zr	1300.0	1500.0	2710.0	2700.0	2000.0	1200.0	940.0	7340.0	1000.0	1610.0
Ba	3200.0	1800.0	6400.0	8400.0	1000.0	3100.0	700.0	1030.0	900.0	690.0
Zn	87.0	560.0	190.0	190.0	460.0	97.0	60.0	1300.0	30.0	57.0
Ce	70.0	54.0	39.9	39.9	20.0	50.0	44.0	77.0	42.0	58.0
Pb	36.0	867.0	41.0	31.0	24.0	26.0	9.1	47.0	25.0	84.0
Bi	0.2	0.9	0.3	0.0	10.0	0.1	1.0	2.0	0.9	0.5
Ga	40.0	12.0	9.1	9.0	4.0	39.0	19.9	31.0	22.0	26.0
As	47.0	17.0	6.0	6.0	4.1	7.0	11.0	4.0	15.0	15.1
Y	75.0	3.9	20.0	20.0	19.0	15.0	28.0	87.0	15.0	2.9
Ir	22.0	6.1	1.0	1.0	4.6	20.0	30.0	5.6	3.1	2.1
Au	0.3	0.5	0.4	0.4	1.9	0.2	0.0	0.0	0.2	0.4
Ni	0.0	<0.001	<0.001	0.0	0.0	<0.001	<0.001	0.0	0.0	<0.001
Rb	30.0	30.0	86.0	86.0	47.0	29.0	5.5	13.0	30.0	39.0
Mo	32.0	83.0	0.0	0.0	0.0	32.0	40.0	11.0	48.0	18.0
Co	0.0	0.2	0.3	0.3	0.0	0.0	<0.001	0.0	0.0	<0.001
Cd	0.0	1.1	0.0	<0.001	<0.001	0.0	0.3	1.0	1.0	5.0
Ru	0.0	<0.001	8.7	8.7	1.0	0.0	0.0	<0.001	0.0	<0..001
Eu	0.1	2.1	31.0	30.0	33.0	0.2	1.0	4.4	1.3	8.6
Re	170.0	34.0	0.0	0.0	<0.001	180.5	16.0	23.0	120.0	38.0
Nb	30.8	35.0	24.1	24.1	20.0	30.0	13.8	20.0	40.0	30.0
Ag	0.4	0.1	1.3	1.3	0.5	0.4	0.6	1.4	1.1	1.2
Ta	42.1	64.0	64.1	64.1	15.0	42.1	61.0	40.2	36.0	41.2
W	0.9	1.5	4.0	4.0	2.5	0.9	6.1	12.3	1.0	0.9
Hf	33.0	21.0	14.0	14.0	9.1	33.0	20.4	18.1	20.0	11.0
Yb	4.0	6.9	1.0	1.0	2.3	4.0	0.1	0.5	2.1	5.9
In	2.1	0.1	5.2	5.2	1.8	2.1	2.3	4.1	1.9	8.0
Se	0.0	0.0	0.3	0.3	<0.001	<0.001	0.2	0.1	0.2	<0.001
U	<0.001	0.0	0.2	0.2	0.0	<0.001	0.0	<0.001	0.0	<0.001
Th	2.5	2.2	0.2	0.2	0.2	2.5	0.3	1.0	0.9	0.2
Sb	7.0	14.0	0.3	0.3	1.1	7.0	4.0	12.0	6.8	3.2
Ge	24.0	44.0	8.6	90.6	4.4	20.0	8.5	4.2	4.0	68.0
Sn	30.3	21.1	47.2	47.2	21.1	31.1	47.3	40.7	17.2	43.4

4.2. Geochemistry

Representative samples selected from the study area were analyzed. Major and trace elements were determined for selected morphological form of migmatites. The analyses were carried out on pressed powdered pellets rock samples. The concentration of the major elements is expressed in wt. % is while the concentration of the trace element is expressed in ppm as shown in Tables 6 and 7.

4.2.1. Variation diagrams

Harker variation diagrams are used to understand the processes occurring during the evolution of magmas. The correlation patterns between selected elements provide an indication in this regard since they are generally related to mixtures of magmas, addition or subtraction of solid phases by contamination or fractional/partial melt crystallization (Fig. 14).

In the case of partial melting the correlation patterns are controlled by the geochemistry of the solid phases that are being added to the melt. In the case of fractional crystallization with assimilation, the patterns of correlation show variability which is related to the inclusion of country rock in the magma during fractionation (Rollinson, 1993). In this case we are dealing with metamorphic rocks i.e. the case of partial melting.

4.2.2. HSFE element variation diagram

The recognition that REE, Y, Th and U-rich accessories minerals may play an important role in controlling the geochemistry of crustal melts is well established (e.g. Watson, 1988; Watt et al., 1996; Bea, 1996; Sawyer, 2008). Crustal rocks always contain REE, Y, Th, U-rich accessory minerals which usually account for an elevated fraction of REE, Y, Th and U contents in bulk rock (e.g. Gromet and Silver, 1983; Sawka, 1988) and may therefore disturb or even completely mask the effects produced by major minerals during melting and crystallization (Bea and Montero, 1999) and may therefore disturb or even completely mask the effects produced by major minerals during melting and crystallization.

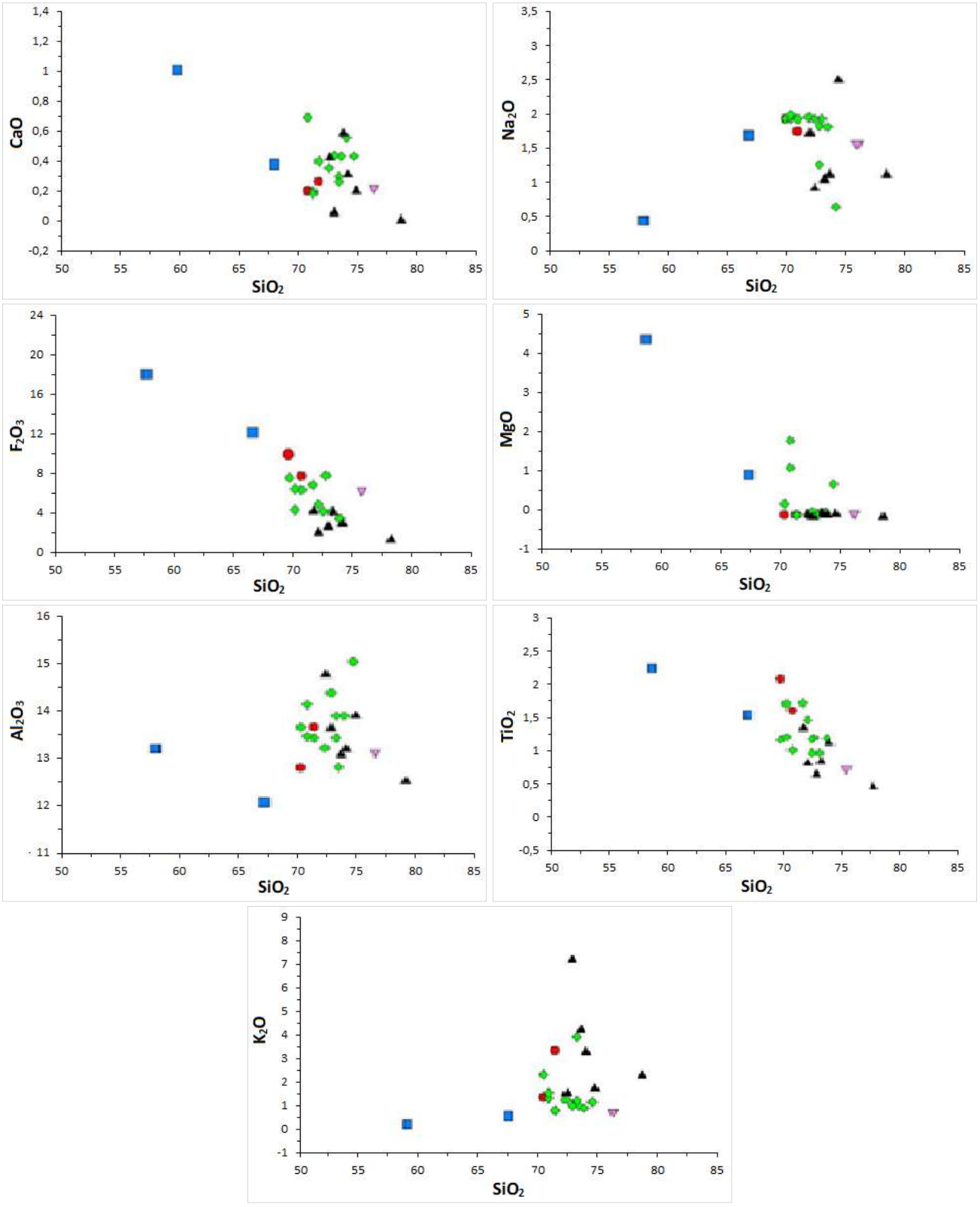

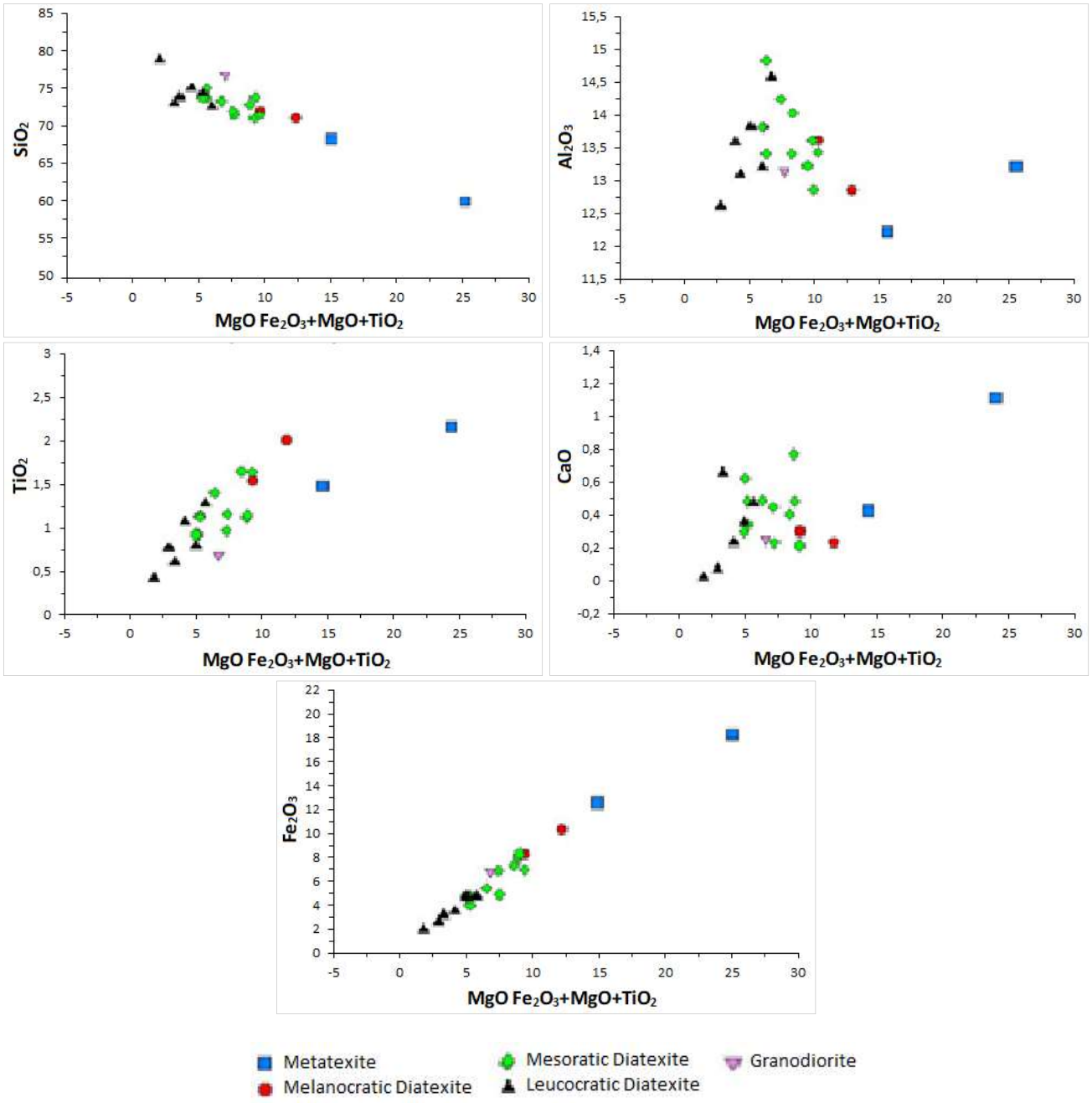

Fig. 14. Harker diagrams for the rocks projecting major elements versus silica content and major elements versus ferromagnesian component

The geochemistry of HSFE reflects the behaviour of accessories and some key major minerals such as garnet, feldspars and amphibole, and may therefore give valuable information about the conditions of partial melting, melt segregation and crystallization of granite magmas in different crustal regimes (Bea, 1996).

4.2.3. Multielement diagram

On a primitive mantle-normalized multi-element variation diagram (Taylor and McLennan, 1985), all samples are characterized by pronounced negative Rb-Y-P anomalies. An exception for the metatexite sample with pronounced negative Sr anomaly. Over all the studied samples are characterized by depleted of large ion lithophile elements (Rb, K and Ce) with the exception of Ba which increases and enrichment high field strength elements (Hf, and Ti) but the high field strength element Zr was relatively Increases, Y was slightly depleted and P strongly depleted (Fig. 17).

4.2.4. Classification

The B-A diagram as proposed by Debon and Le Fort (1983) with classification fields for various types of peraluminous rocks designed by Villaseca et al. (1998) (Fig. 18). The B = Fe+Mg+Ti parameter reflects the content of mafic minerals and the A = Al-(K+ Na+2Ca) parameter reflects the amount of aluminum incorporated into feldspars (calculations are based on millications). All the rocks from the study area plot in the peraluminous domain. They all fall in the highly peraluminous field. Diagram Na-K-Ca of Raju and Rao (1972) ternary diagram (Fig. 19), demarks the field of granitic

rocks originated by magmatic processes from granitic rocks originated by metamorphic/metasomatic processes. In general, the rocks from the study area plot close to or in the metamorphic/metasomatic fields. Rb-Ba-Sr diagram proposed by el Bouseily and el Sokkary (1975) in (Fig. 20) classification scheme was used to determine the relationship between Rb, Ba, Sr in granitoids.

It is used to define part of differentiation in granitic series as well as to distinguish between rocks formed exclusively by magma from those formed by metasomatism or in intimate assocaiation with the host rocks (anomalous granite). The metatexites plotted in the dioritic field while all the diatexites fall from granite to Anomalous granite to Granodioritic Field.

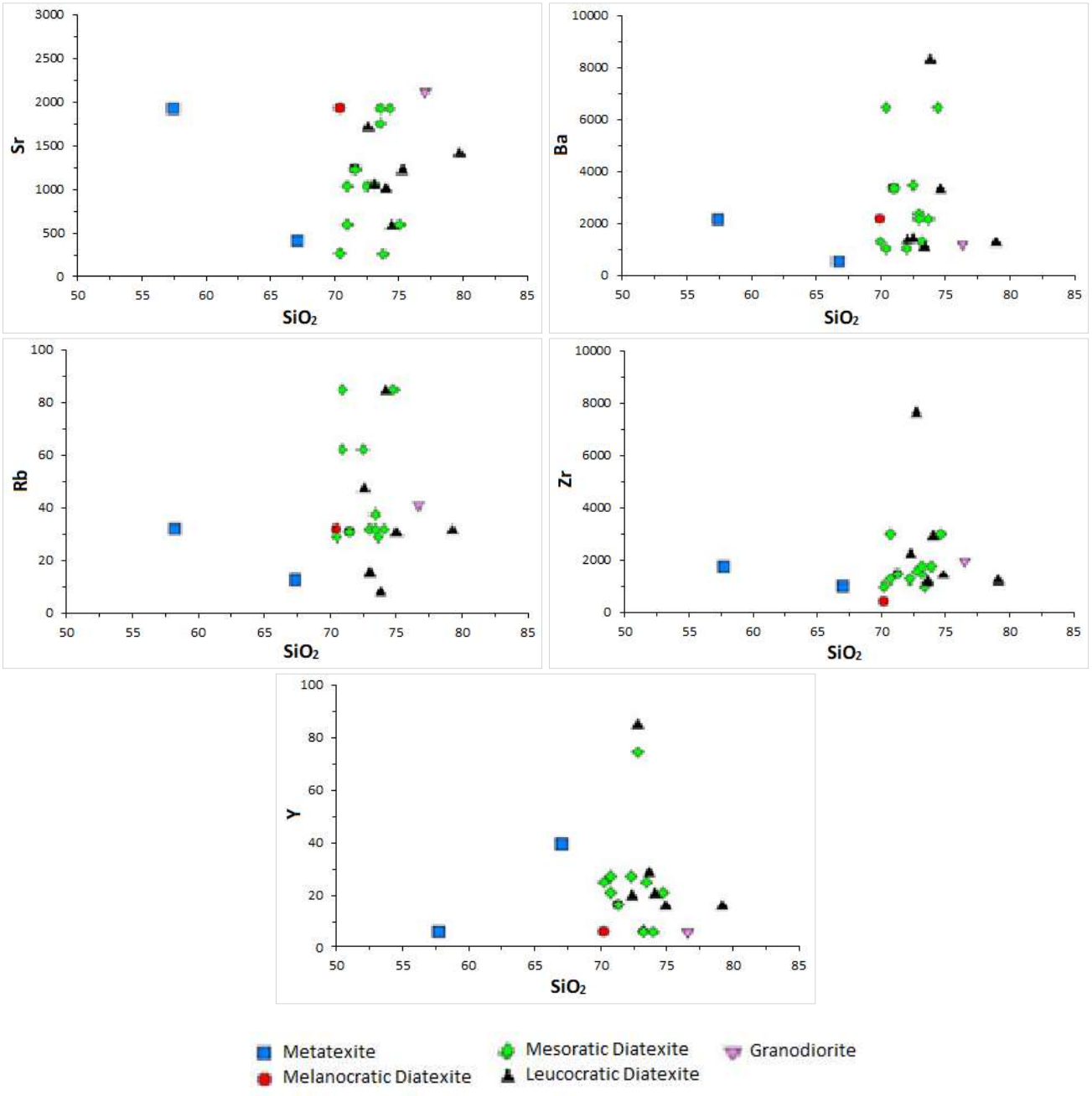

Fig. 15. Harker diagrams for the rocks projecting major elements versus selected trace elements

Total Alkali Silica diagram, as proposed by Cox et al. (1979), use to classify plutonic rock using SiO2 Vs Na2O+K2O. In the TAS diagram (Fig. 21), metatexite show diorite to granodioritic composition, the melanocratic diatexite and mesocratic diatexite, and granodiorite are plotted in the Granodiorite to Granite field, while Leucocratic Diatexite tends to granite field.

4.2.5. Tectonic discrimination

Several authors (Batchelor and Bowden, 1985; Foster et al. 2001; Pearce et al., 1984) consider that magmas produced in different tectonic environments can be distinguished based on their chemical composition. Batchelor and Bowden (1985) propose a tectonic environ-ment discrimination considering the parameters R1 and R2 based on major elements (Fig. 25).

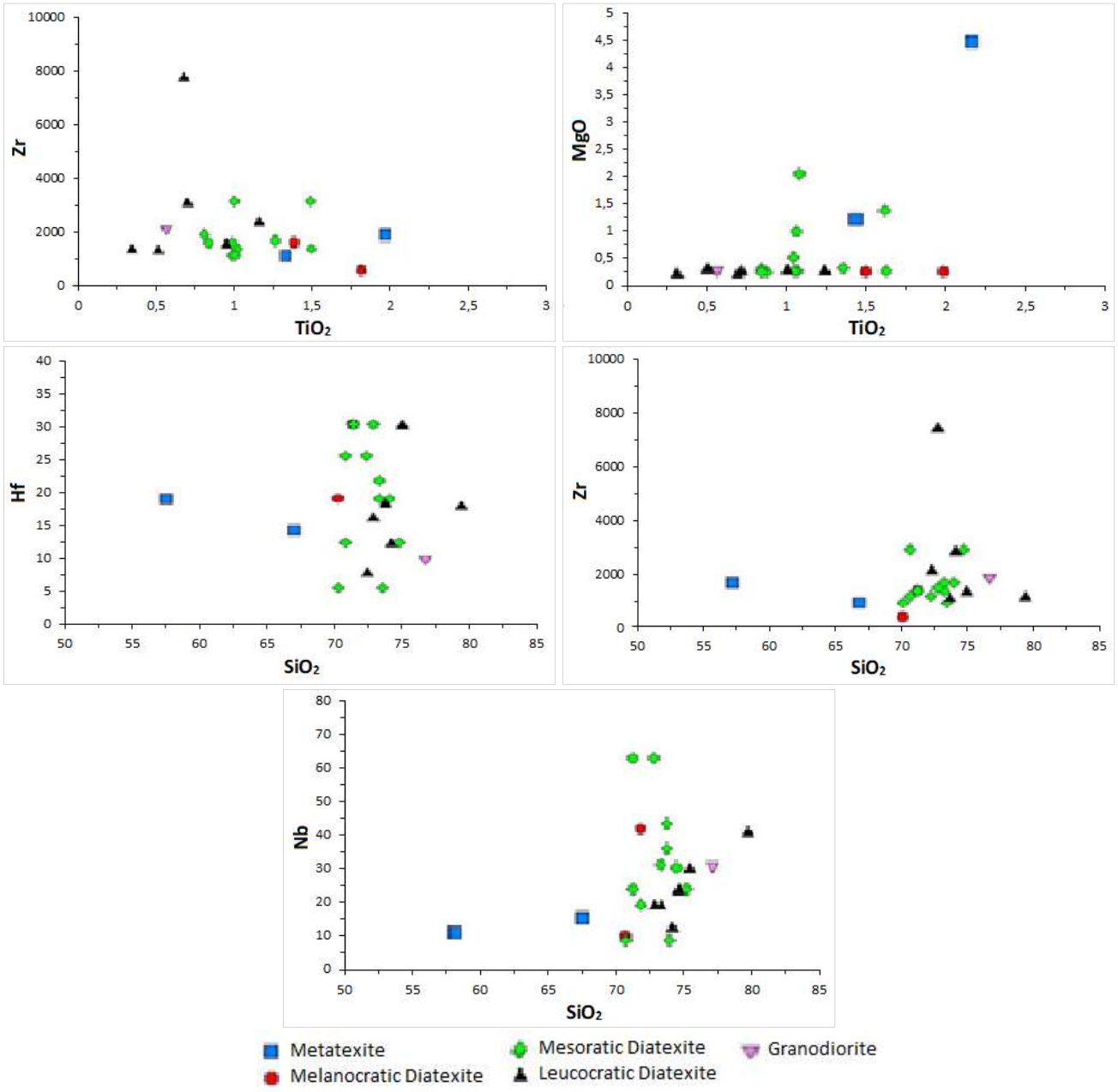

Fig. 16. Variation diagrams for the rocks projecting TiO_2 Vs Zr, TiO_2 Vs MgO, SiO_2 Vs Hf, SiO_2 Vs Zr, and SiO_2 Vs Nb

Triangular diagram with apices Hf, Rb/30 and Ta*3, proposed by Harris et al. (1986) for classification of collisional granites. (Fig. 26). Pearce et al. (1984), suggest a set of diagrams using HFSE such as Ta, Zr, Y and Nb that are the most stable under various conditions and hydrothermal metamorphism (Fig. 27). For granitic rocks these authors proposed distinguish four kinds of tectonic environment: ORG-granites of oceanic rift, fore-arc and back-arc; VAG-oceanic volcanic arc and active margins granites; WPG-within plate granites in attenuated crust and island arcs; COLG-collisional granites, syn-tectonic, associated with continent-continent collision and continent-arc.

5. Discussion

5.1. Field relationship

The study area is underlain by two major rock types, metatexite and diatexites. The metatexites in the study area are patch metatexites (Fig. 6).

This texture is seen when melting occurs at discrete sites to form small, scattered patches of non-foliated in situ neosome. Patch migmatites are rare and in this case they occur with diatexites as patches. They are dominated by paleosome and are characterized by the occurrence of small scattered patches of leucosome resulting from discrete partial melting. The diatexites found in the study area show a considerable range in morphology from mesocratic to melanocatic through to leucocratic diatexites (Figs. 8 and 9).

5.2. Petrography

The different morphological form of migmatites in the studied area are petrographically studied carefully with the use of a microscope, the mineralogical features exhibited by the minerals are observed both under Plane Polarized light (PPL) and Cross Polarized Light (XPL).

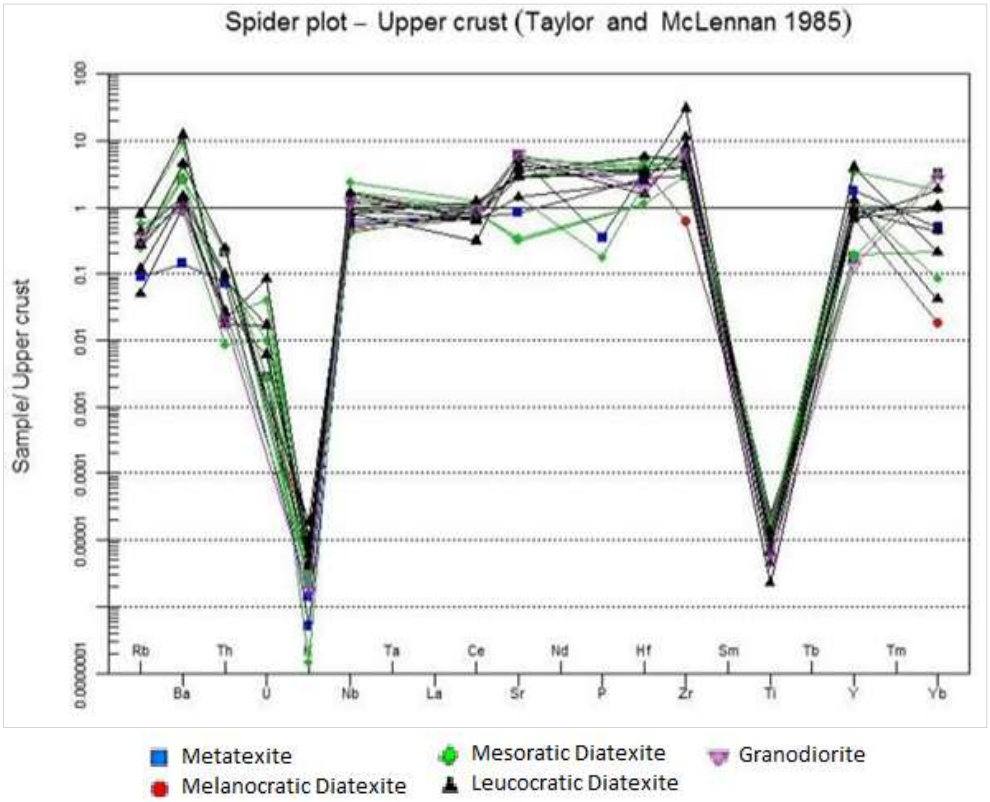

Fig. 17. Primitive mantle normalized plot of incompatible trace elements for samples of migmatitic rocks from different migmatitic suites of the study areas after (Taylor and McLennan, 1985)

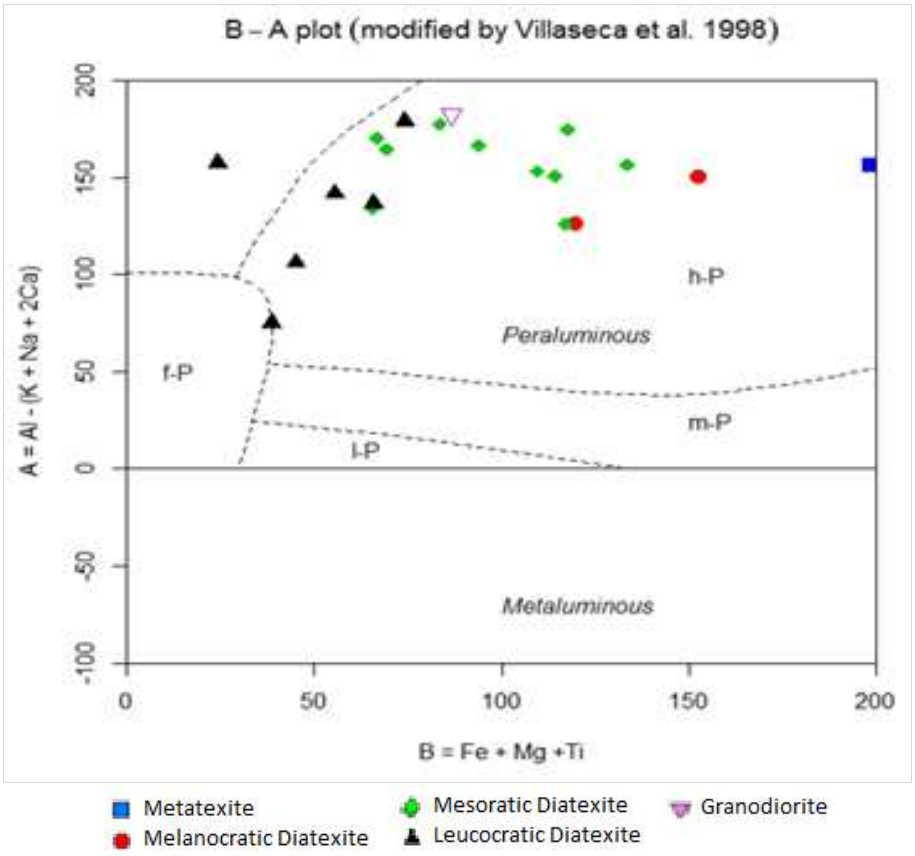

Fig. 18. B-A diagram as proposed by Debon and Le Fort (1983) modified after Villaseca et al. (1998). Abbreviations: l-P = Low peraluminous; mP – moderate peraluminous; h-P – high peraluminous and f-P felsic peraluminous

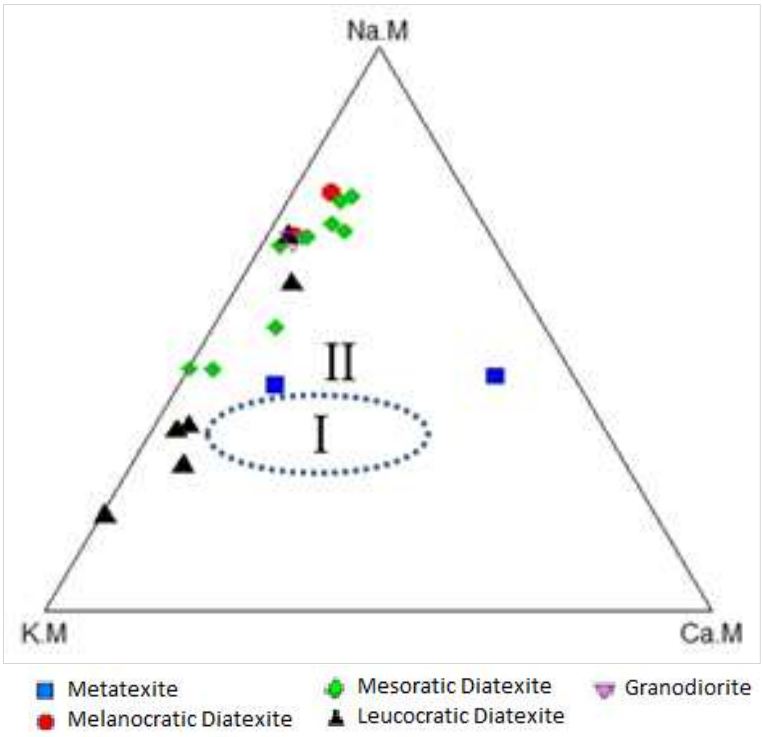

Fig. 19. Diagram Na-K-Ca (in milications) of Raju and Rao (1972). Fields: I - magmatic granitic rocks; II – replacement granites rocks

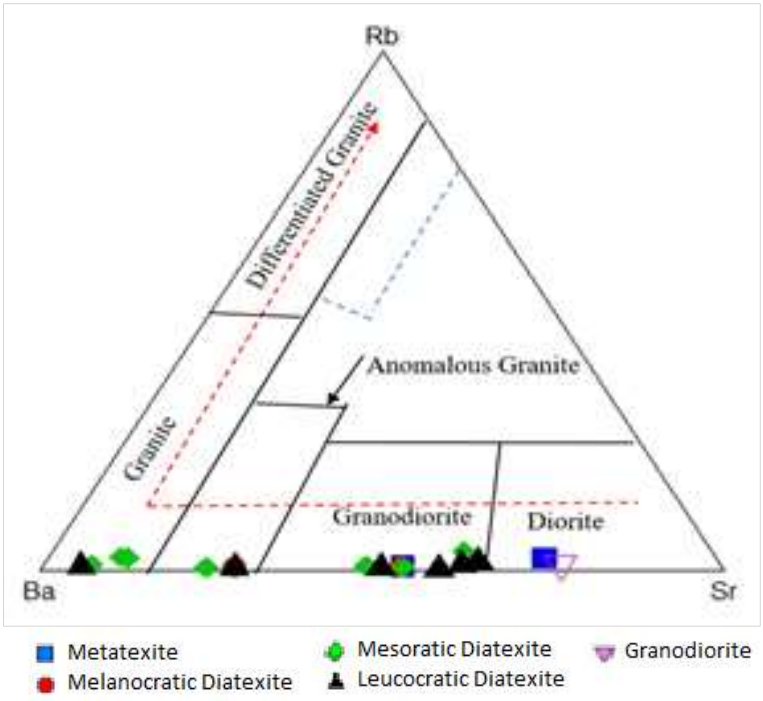

Fig. 20. Rb-Ba-Sr diagram of El Bouseily and El Sokkary (1975)

The metatexites comprise of quartz + plagioclase + biotite +orthopyroxene + silliminite + accessory minerals and a typical abundance of orthopyroxene and biotite. Quartz is generally equant and polygonal in the orthopyroxene-dominated part and exhibits conspicuous undulose extinction and irregular grain boundaries (Fig. 7). The biotites are elongated with prismatic shape (Fig. 7). Strongly pleochroic orthopyroxene surrounded by plagioclase, quartz, and biotites is present (Fig. 7). The schistosity is defined principally by the preferred orientation of biotite. The metatexites are generally medium to fine grained (0.7-1 mm) rocks with granoblastic-polygonal microstructures (Fig. 7).

The granolepidoblastic texture is largely defined by the biotite quartz association, and frequently have matrix mineral inclusions, such as biotite, quartz and ilmenite.

The melanocratic diatexite have granoblastic texture and is composed of plagioclase, biotite, K-feldspar, and quartz. It contains predominantly the ferromagnesian minerals; there is Garnet porphyroblast in the rock matrix (Figs. 10 and 11).

The mesocratic diatexite is principal of plagioclase, K-feldspar, orthopyroxene, biotite, and quartz, and the texture is granoblastic. The plagioclase shows albite twinning and some shows sign of deformation or strain (Figs. 12 and 13).

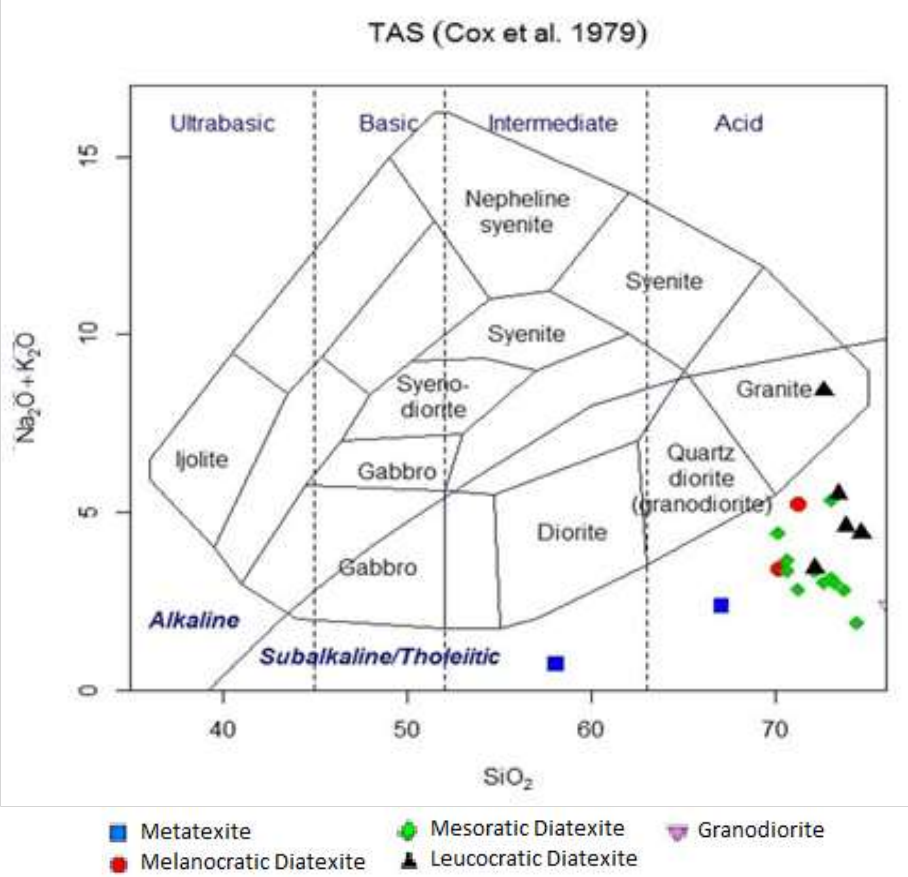

Fig. 21. Total Alkali Silica diagram proposed by Cox et al. (1979)

The biotite is dark brown and abundant while the microcline grains exhibit obliterated cross-hatched twinning. Quartz occurs in large masses showing a varying degrees of strain extinction and exhibits undulose extinction.

Fibrolitic sillimanite occurs within the Mesocratic diatexite, associated with biotite and skirting the matrix grains. Petrographic analysis shows that the Leucocratic diatexite has a granoblastic texture and is composed of biotite, K-feldspar, and quartz. It contains predominantly the felsic minerals; the quartz is predominant in terms of modal composition proportionate to microcline.

Quartz occurring principally in large irregular masses may show strain effects. Mesocratic diatexites and leucocratic diatexites show myrmekite intergrowths, in most of the cases associated with micas or sillimanite suggesting a relationship between the biotite melting reactions and the occurrence of myrmekite. There are myrmekites protruding into K-feldspar crystals but most of them occur as inclusions both in K-feldspar and in quartz large crystals. Patchy perthites in K-feldspar, slightly deformed plagioclase and quartz crystals showing undulose extinction are evidence of ductile shearing deformation processes affecting these rocks.

The presence of metamorphic optical properties such as undulous extinction in quartz and obliteration of twinning in feldspar, and microstructure such as mymerkite, perthite indicate the rocks were subjected to pressure and temperature, and that partial melting is the main process that form the different suites of Migmatitic and associated rocks of the study area.

5.3. Geochemistry

5.3.1. Major element

The metatexites, melanocratic diatexite, mesocratic diatexite, leucocratic diatexite and granodiorite are compositionally different in their mean values as revealed by major oxide data presented in Tables 6 and 7.

The lowest mean value of SiO_2 is w = 62.58 % which indicates the mafic nature of the metatexites while the mean value of SiO_2 is w = 70.66 % for the melanocratic diatexite and SiO_2 is w = 71.81 % for mesocratic diatexite and the highest mean value of SiO_2 is w = 74.21 % which as well reveal the felsic nature of the leucocratic diatexite, the granodiorite has SiO_2 is w = 76.2 %.

The ferromagnesian elements content is low in leucocratic diatexite ~3.12 and increasingly for mesocratic diatexite ~5.04, melanocratic diatexite ~9.06 and the highest been for metatexite ~15.3. K_2O content (metatexite ~0.4 melanocratic diatexite ~2.41 mesocratic diatexite ~2.04 and leucocratic diatexite ~2.4). CaO content (metatexite ~0.7 melanocratic diatexite ~0.23 mesocratic diatexite ~0.23 and leucocratic diatexite ~0.16). Leucocratic diatexite show the lowest ferromagnesian, HSFE and TiO_2 contents, high variation in K_2O content and high Na_2O and Ba contents. Considering the lithologies independently or considering the migmatitic rocks as a whole there are no evident correlations between major or trace elements and the silica content (Figs. 6 and 7). Only a slight correlation between SiO_2 and some oxides is observed. This suggests that the classic model of fractional crystallization is not the principal process influencing the lithological diversity.

In Harker variation diagrams (Fig. 6) for most of the samples: MgO, Fe_2O_3, Al_2O_3, CaO, P_2O_5 and TiO_2 decrease with increasing SiO_2 contents even though some shows scattered distributions. Because MgO, CaO, Fe_2O_3 and TiO_2 take part in ferromagnesian minerals formation in initial steps of partial melting and metamorphic crystallization, so their concentration and trace elements decreases with increasing (Fig. 14) in SiO_2 contents.

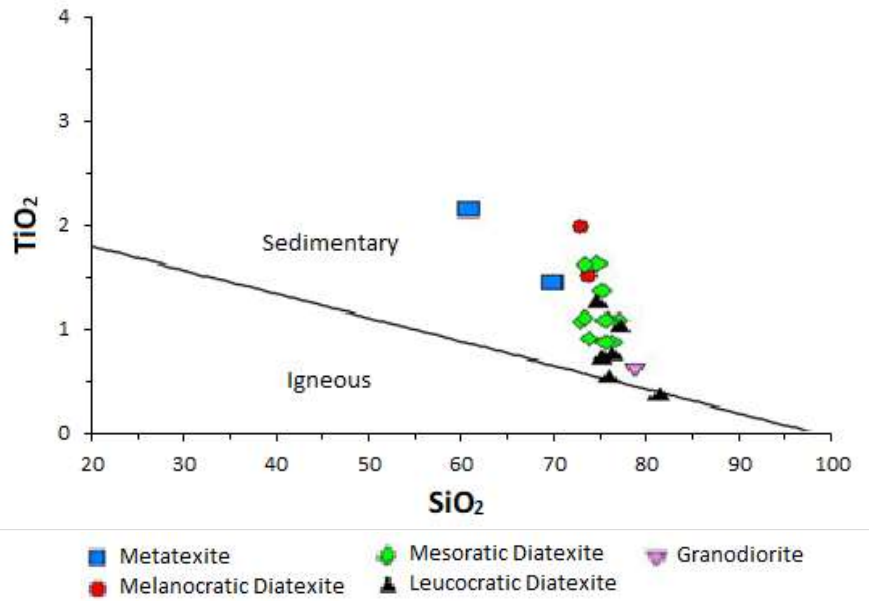

Fig. 22. K_2O/Al_2O_3 versus Na_2O/Al_2O_3 diagram after (Garrels and Mackenzie, 1971)

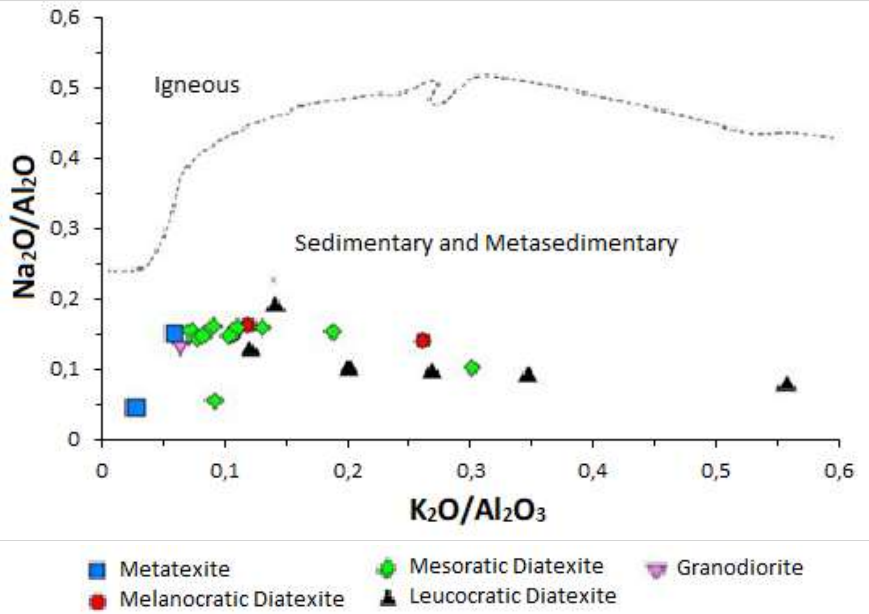

Fig. 23. TiO_2 versus SiO_2 plot after (Tarney, 1977)

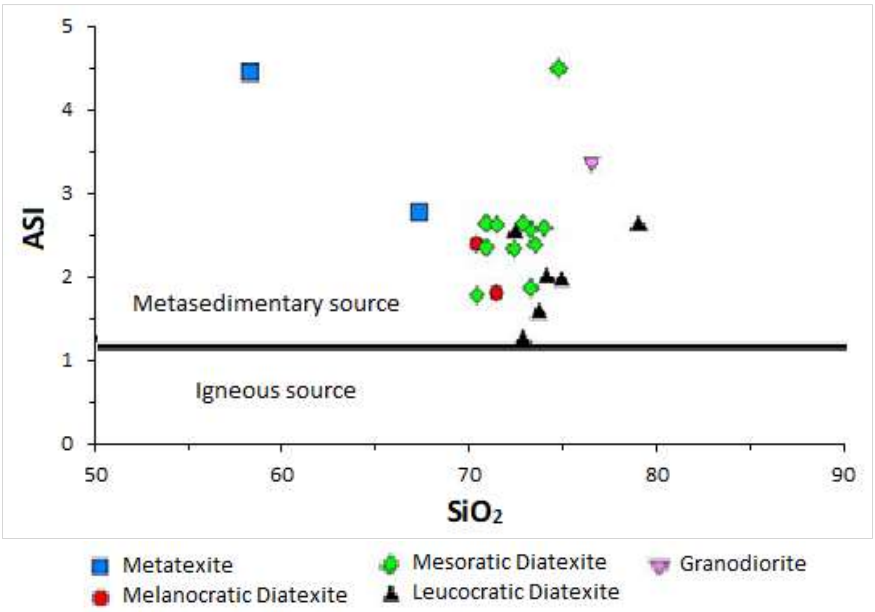

Fig. 24. SiO_2 versus Al_2O_3/ (CaO + Na_2O + K_2O) diagram after Clarke et al. (2005)

The case of partial melting, the correlation patterns are controlled by the geochemistry of the solid phases that are being added to the melt. In this case we are dealing with metamorphic rocks i.e. the case of partial melting. The patterns defined by major and selected trace elements versus the content in Ferromagnesian components (Fe_2O_3 + MgO + TiO_2) for the rocks in the study area (Figs. 14 and 15). A notable feature is the positive correlation between TiO_2, Fe_2O_3, CaO and HSFE content and the content in Ferromagnesian minerals (in this case biotite since it is the only mineral that contains Fe_2O_3, MgO and TiO_2 in these rocks).

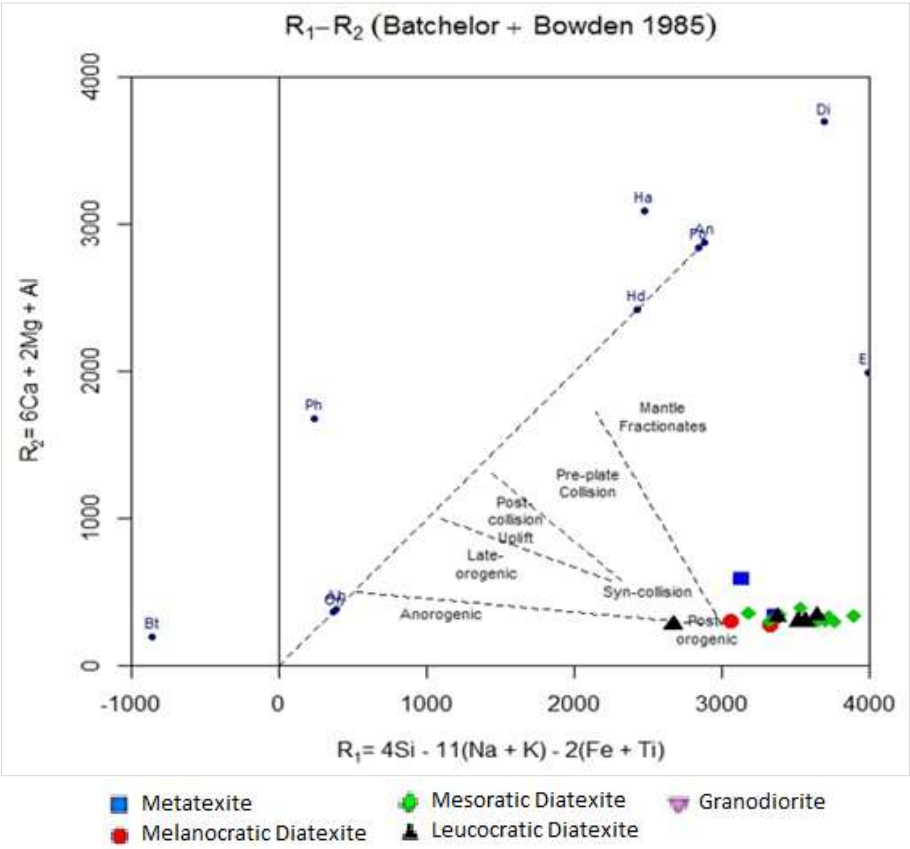

Fig. 25. Tectonic discrimination diagram after Batchelor and Bowden (1985)

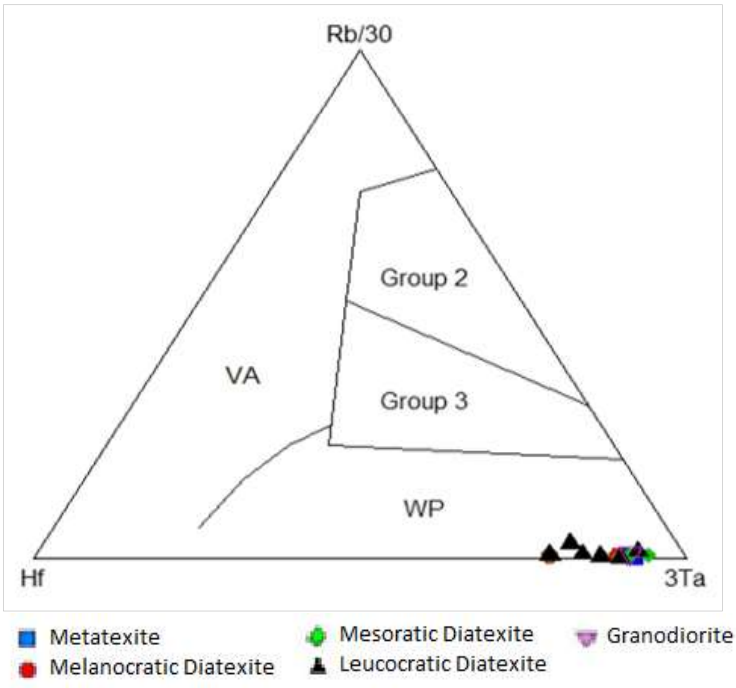

Fig. 26. Triangular diagram with Hf, Rb/30 and Ta*3, proposed by Harris et al. (1986)

In contrast, the elements compatible in reactant phases during the melting processes (Rb, Ba and Sr) show a higher range of variation (Figs. 14 and 15) with no clear correlation with mafic components. These elements are concentrated in minerals that are key reagents in the melting reactions that produce granites, e.g., biotite, quartz, plagioclase and garnet (Sawyer, 2008).

The geochemistry of HSFE (Fig. 16) reflects the behaviour of accessories and some key major minerals such as garnet, feldspars and amphibole, and therefore give valuable information about the conditions of partial melting, melt segregation and crystallization of granite magmas in different crustal regimes.

On a primitive mantle-normalized multi-element variation diagram (Fig. 17) all samples are characterized by pronounced negative Rb-Y-P anomalies. An exception for the metatexite sample with pronounced negative Sr anomaly. Over all the studied sa ew3mples are characterized by depleted of large ion lithophile elements (Rb, K and Ce) with the exception of Ba which increases and enrichment high field strength elements (Hf, and Ti) but the high field strength element Zr was relatively Increases, Y was slightly depleted and P strongly depleted.

5.3.2. Classification

The B-A diagram as proposed by Debon and Le Fort (1983) with classification fields for various types of rocks designed by Villaseca et al. (1998) shows all the samples from the study area plot in the peraluminous domain (Fig. 18). They all fall in the highly Peraluminous field.

Diagram Na-K-Ca of Raju and Rao (1972), shows the rocks from the study area plot close to in the metamorphic/ metasomatic fields (Fig. 19).

Rb-Ba-Sr diagram proposed by El Bouseily and El Sokkary (1975) in (Fig. 20) classification scheme was used to determine the relationship between Rb, Ba, Sr in granitoids. It is used to define part of differentiation in granitic series as well as to distinguish between rocks formed exclusively by magma from those formed by metasomatism or in intimate assocaiation with the host rocks (anomalous granite). The Metatexites plotted in the dioritic field while all the diatexites fall from granite to Anomalous granite to Granodioritic Field.

Based on Total Alkali Silica classification Cox et al. (1979), Metatexite show diorite to granodioritic composition, the Melanocratic Diatexite and Mesocratic Diatexite are plotted in the Granodiorite to Granite field, while Leucocratic Diatexite and Granodiorite tends to granite field (Fig. 21).

Various models were used to determine the Protolith of the migmatite. The K_2O/Al_2O_3 vs Na_2O/Al_2O_3 plot was used to discriminate between igneous and sedimentary/ metasedimentary rocks after (Garrels and Mackenzie, 1971). All the plots fell within sedimentary/ metasedimentary field (Fig. 22). TiO_2 vs SiO_2 diagram after (Tarney, 1976), the plot (Fig. 23) fell within sedimentary field which suggests that the protolith of the migmatite are from partial melting of crustal rocks. Clarke et al. (2005) diagram (Fig. 24) distinguishes between lithologies as either they are derived from metasedimentary source or igneous according to whole-rock major elements chemistry based on SiO_2 vs. ASI and their proportion reflects the sedimentary evolution.

In the Batchelor and Bowden (1985) tectonic environment discrimination all the samples plotted around the post orogenic and syn-collisional field (Fig. 25). In the Harris et al. (1986), all the samples fall on the field of Within Plate Granite (Fig. 27). In the Pearce et al. (1984) diagrams most

of the samples fall between Within plate granites in attenuated crust and island arcs and collisional granites, syn-tectonic, associated with continent-continent collision and continent- arc (Fig. 19).

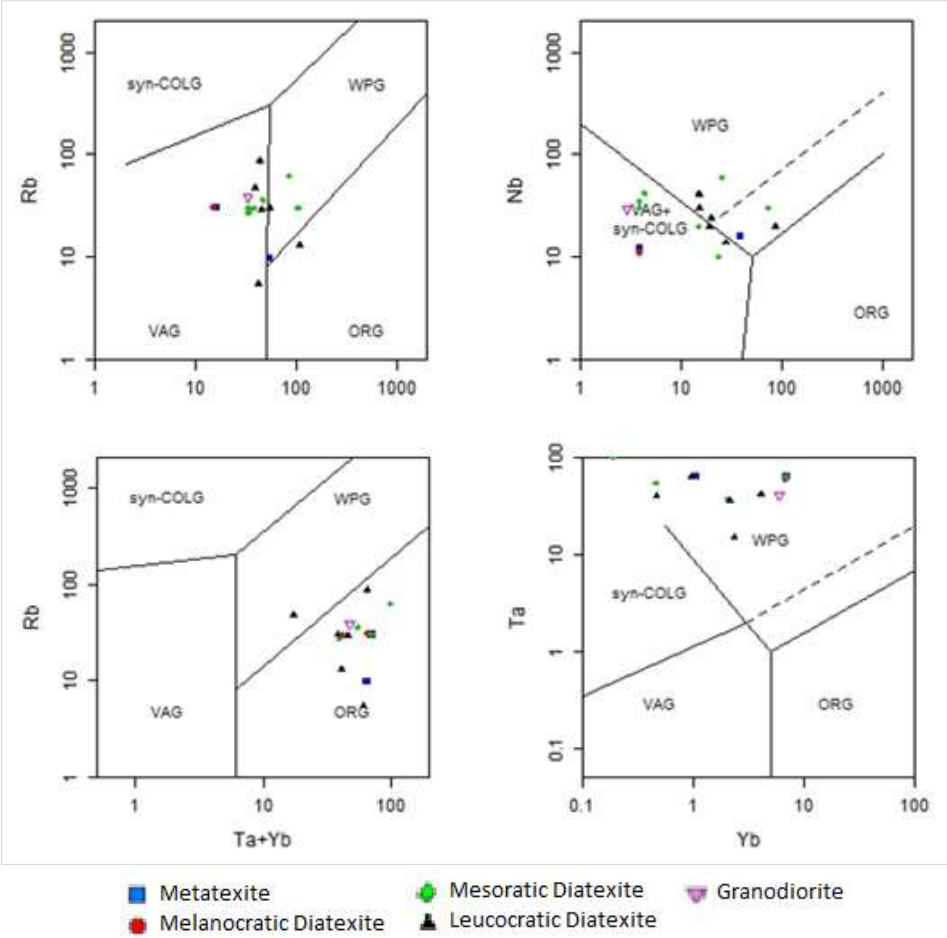

Fig. 27. Geotectonic environment of the granitoid rocks proposed by Pearce et al. (1984)

6. Conclusion

The integration of geochemical data, petrography and field/morphological data, evaluation of several parameters of the study area from the geochemical data and petrography the following conclusions can be drawn:

1. The study area has various morphological units of migmatites, that are mainly metatexite (patchy type), diatexite (melanocratic diatexite, mesocratic diatexite, and leucocratic diatexite) and granodiorite that are intricately associated with one another and the metatexite occurring as patches within the diatexite and all the diatexites melanocratic, mesocratic and Leucocratic diatexites having clear contact relationship with each other and the Granodiorites occurring as massive boulders adjacent to the migmatitic Rocks.

2. The presence of petrographic properties such as undulouse extinction in quartz, preferred elongation platy Biotite, Metamorphic minerals like orthopyroxenene, Silliminite and Microstructures like the Mymerkites and Pertithes, indicate the study area to be a metamorphic terrain that has undergone shearing. The grade of metamorphism increases from metatexites, which is indicated by preferred elongation of biotite and abundance of orthopyroxenes, through to the diatexites, which is indicated by the general coarsening of quartz grain size and absentia of these properties.

3. The textural and compositional evidence suggest that the dominant process for generating the migmatites in the study area was partial-melting. Textural evidences of partial melting processes are widespread both in metatexites and in diatexitic rocks. Moreover, the abundance of biotite and plus or minus orthopyroxene and silliminite confirm to this. So also Harker variations diagrams in the correlation pattern are controlled by the geochemistry of solid phases that are being added to the melt.

4. The rocks show S-type affinity (highly peraluminous), with high content of SiO_2, Al_2O_3 and Fe_2O_3 and low content of CaO, MgO.

5. From Geochemical plot of several discrimination diagrams of Tectonic environment that shows Within Plate Granites or Syn-collisional field in attenuated crust and island arcs and collisional granites, syn-tectonic, associated with continent-continent collision and continent- arc we can say that the rocks were produce Continent-Continent

collision i.e. the Himalayan type collision and so also by their affinity that they are highly peraluminous showing their S-type signature.

6. The metatexites exposed in the area have been deformed from amphibolite facies metamorphic conditions, whereas the diatexites were in granulite facies condition typified by granulite mineral assemblages.

7. Field relationships, petrography, whole-rock chemistry shows that all the morphological forms of migmatite, metatexite occurring as patch metatexite, diatexite as melanocratic, mesocratic and leucocratic diatexite, granodiorite (Nebulite) have the same protolith of sedimentary/metasedimentary and the cause of lithological diversity and heterogeneity is the transformation process from one morphological form to another.

Acknowledgement
The author greatly indebted to Prof. Ahmed Isah Haruna, Department of Applied Geology Abubakar Tafawa Balewa University Bauchi, Nigeria for his constructive comment and mentorship leading to important improvement of this work and for introducing me to the fascinating and mystifying world of migmatite and also to my immediate family and friends for helping me throughout this task. This publication is derived from part of my MSc. thesis. I would like to acknowledge the effort of my family and friends for making this all possible. Thank you all and God bless.

Statements and Declarations
The authors declare that no funds, grants, or other support were received during the preparation of this manuscript. The authors have no relevant financial or non-financial interests to disclose. All authors contributed to the study conception and design. The draft of the manuscript was written by Tahir Garba Ahmad and all authors commented on the manuscript. All authors have read and approved.

References

Abaa, S.I., 1983. The structure and petrography of alkaline rocks of the Mada Younger Granite Complex, Nigeria. Jounal of African Earth Science 3, 107-113.

Ajibade, A.C., Fitches, W.R., Wright, J.B., 1979. The Zungeru mylonites, Nigeria: recognition of amajor unit. Revue de Géologie et Géographie Physique 21, 359-363.

Ajibade, A.C., Wright, J.B., 1989. The Togo–Benin–Nigeria Shield: Evidence of crustal aggregation in the Panafrican Belt. Journal of Tectonophysics 165, 125-129.

Ball, E., 1980. An example of very consistent brittle deformation over a wide intra- continental area: the late Pan-African fracture system of the Tuareg and Nigerian shield. Tectonophys 61, 363-379.

Barley, M.E., Eisenlohr, B.N., Groves, D.I., Perring, C.S., Vearncombe, J.R., 1989. Late Archaean convergent margin tectonics and gold mineralization: a new look at the NorsemanWilunaBelt, Western Australia. Geology 17, 826-829.

Batchelor, R.A., Bowden, P., 1985. Petrogenetic inter-pretation of granitoid rock series using multicationic parameters. Chemical Geology 48, 43-55.

Bea, F., 1996. Residence of REE, Y, Th and U in granites and crustal protoliths: Implications for the chemistry of crustal melts. Journal of Petrology 37, 521-552.

Bea, F., Montero, P., 1999. Behavior of accessory phases and redistribution of Zr, REE, Y, Th, and U during metamorphism and partial melting of metapelites in the lower crust: An example from the Kinzigite Formation of Ivrea-Verbano, NW Italy.Geochimica et Cosmochimica Acta 63, 1133-1153.

Black, R., Caby, R., Moussine-Pouchkine, A., Bayer, R., Betrand, J. M., Boullier, M.M., Fabre, J., Resquer, A., 1979. Evidence for late Precambrian plate tectonics in West Africa. Nature 278, 223-227.

Black, R., Girod, M., 1972. In African Magmatism and Tectonics (eds Clifford, T.N., Gass, I.G.,) 185-210. (Oliver and Boyd, Edinburgh 1972).

Burke, K.C., Dewey, F.J., 1972. Orogeny in Africa. In: Dessauvagie, T.F.J. and Whiteman, A.J., Ed., African Geology, Ibadan University Press, Ibadan, 583-608.

Caby, R., Bertrand, J.M.I., Black, R., 1981. Pan African Ocean Closure and Continental Collision in the HoggarIforas Segment, Central Sahara. In: Kroner, A., Ed., Precambrian Plate Tectonics, Elsevier, Amsterdam, 407-434.

Clarke, D.B., Dorais, M., Barbarin, B., Barker, D., Cesare, B., Clarke, G., el Baghdadi, M., Erdmann, S., Förster, H.J., Gaeta, M., Gottesmann, B., Jamieson, R.A., Kontak, D.J., Koller, F., Gomes, C.L., London, D., Morgan, VI. G.B., Neves, L.J.P.F., Pattison, D.R.M., Pereira, A.J.S.C., Pichavant, M., Rapela, C.W., Renno, A.D., Richards, S., Roberts, M., Rottura, A., Saavedra, J., Sial, A.N., Toselli, A.J., Ugidos, J.M., Uher, P., Villaseca, C., Visonà, D., Whitney, D.L., Williamson, B., Woodard, H.H., 2005. Occurrence and origin of andalusite in peraluminous felsic igneous rocks. Journal of Petrology 46, 441-472.

Cox, K.G., Bell, J.D., Pankhurst, R.J., 1979. The Interpretation of Igneous rocks. George Allen and Unwin, London.

Dada, S.S., 2006. Crust forming ages and Proterozoic crustal evolution in Nigeria, a reappraisal of current interpretations. Precambrian Research 87, 65-74.

Debon, F., Le Fort, P., 1983. A chemical–mineralogical classification of common plutonic rocks and associations. Transactions of the Royal Society of Edinburgh, Journal of Earth Sciences 73, 135-149.

El Bouseily, A.M., El Sokkary, A.A., 1975. The relation between Rb, Ba and Sr in granitic rocks. Chemical Geology 16 (3), 207-219.

Ferre, C.E., Caby, R., 2006. Granulite facies metamorphism and charnockite plutonism: examples from the Neoproterozoic Belt of Northern Nigeria. Journal of Geology 100, 06006.

Frost, B.R., Barnes, C.G., Collins, W.J., Arculus, R.J., Ellis, D.J., Frost, C.D., 2001. A geochemical classification for granitic rocks. Journal of Petrology 42, 2033-2048.

Gandu, A.H., Ojo, S.B., Ajakaiye, D.E., 1986. A gravity study of the Precambrian rocks in the Malum-fashi area of Kaduna State, Nigeria. Tectonophysics 126,181-194.

Garrels, R.M., Mackenzie, F.T., 1971. Evolution of sedimentary rocks. W. W. Norton & Co. Inc. New York, 394 p.

Gromet, L.P., Silver, L.T., 1983. Rare earth element distribution among minerals in a granodiorite and their pctrogenetic implications. Geochimica et Cosmochimica Acta 47, 925-940.

Harris, N.B.W., Pearce, J.A., Tindle, A.G., 1986. Geochemical characteristics of collision- zone magmatism. In: Coward, M.P, Ries, A.C (Eds.), Collision Tectonics. Geological Society of London Special Publication 19, 67-81.

Kennedy, W.Q., 1964. The structural differentiation of Africa in the Pan African ±500 Ma. tectonic episode, In: 8th Annual Report of the Research Institute of African Geology, Leeds University, UK, 128.

Mehnert, K.R., 1968. Migmatites and the originof granitic rocks. Developments in Petrology 1. Elsevier, Amsterdam. 393 pp.

Mc Curry, P.J., 1989. A general review of the Geology of the Precambrian to lower Paleozoic rocks of Northern Nigeria. In C.A Kogbe (Editor) Geology of Nigeria. Rockview Limited. Jos. pp13-37.

Oyawoye, M.O., 1972. The basement complex of Nigeria. In: Dessauvagie TFJ, Whiteman AJ (eds) African geology. Ibadan University Press, pp 66-102.

Olayinka, A.I., 1992. Geophysical siting of boreholes in crystalline basement areas of Africa. Journal of African Earth Science 14, 197-207.

Pearce, J. A., Harris, N.B.W., Tindle, A.G., 1984. Trace element discrimination diagram for the tectonic interpretation of granitic rocks. Journal of Petrology 25, 956-983.

Rahaman, M.A., Ocan, O., 1978. On Relationship in the Precambrian Migmatite-Gneiss of Nigeria. Journal of Mining and Geology 15, 23-30.

Raju, R.D, Rao, J.S.R.K., 1972. The chemical distinction between replacement and magmatic granitic rocks. Contributions to Mineralogy and Petrology 35, 169-172.

Rollinson, H., 1993. Using Geochemical Data: evaluation, presentation, interpretation. Longman Group UK Limited.

Sawka, W.N., Chappell, B.W., 1988. Fractionation of uranium, thorium and rare earth elements in a vertically zoned granodiorite: implications for heat production distribution in the Sierra Nevada batholith, California, U.S.A. Geochimica et Cosmochimica Acta 52, 1131-1144.

Sawyer, E.W., 2008. Atlas of migmatites: Quebec, Mineralogical Association of Canada, The Canadian Mineralogist Special Publication 9, 386 p.

Sederholm, J.J., 1907. Om granit och gneisderas uppkomst, uppträdande och utbredning inom urbergeti Fennoskandia. Bull. Commission géologique de Finlande 23, 110 pp.

Sederholm, J.J., 1923. On migmatites and associated Precambrian rocks of southwestern Finland I: The Pellinge region. Bull. Commission géologique de Finlande 58, 158 pp.

Sederholm, J.J., 1926. On migmatites and associated Precambrian rocks of southwestern Finland II: The region around the Barösundsfjärd west of Helsingfors and neighbouring areas. Bull.Commission géologique de Finlande 77, 143 pp.

Tarney, J., 1976. Geochemistry of Archaean high-grade gneisses with implications as to the origin and evolution of the Precambrian crust. In: Windley, B.F. (Ed.), The Early History of the Earth. Wiley, New York, pp. 405-418.

Taylor, S.R., McLennan, S.M., 1985. The Continental Crust: Its Composition and Evolution: Oxford, U.K., Blackwell, 312 p.

Watson, E.B., Liang, Y., 1995. A simple model for sector zoning in slowly grown crystals: implications for growth rate and lattice diffusion, with emphasis on accessory minerals in crustal rocks. American Mineralogist 80, 1179-1187

Watt, G.R., Burns, I.M., Graham, G.A., 1996. Chemical characteristics of migmatites: Accessory phase distribution and evidence for fast melt segregation rates. Contribution to Mineralogy and Petrology 125, 100-111.

Villaseca, C., Barbero, L., Herreros, V., 1998. A re-examination of the typology of peraluminous granite types in intracontinental orogenic belts. Transactions of the Royal Society of Edinburgh, Earth Sciences 89, 113-119.

Wright, J.B., Hastings, D.A., Jones, B.W., Williams, H.R., 1985. Geology and Mineral Resourcesof West Africa. George Allen and Unwin. London,187 pp.